frontiers | Frontiers in Earth Science

TYPE Original Research
PUBLISHED 12 January 2023
DOI 10.3389/feart.2022.966085

Check for updates

OPEN ACCESS

EDITED BY
Gilby Jepson,
University of Arizona, United States

REVIEWED BY
Giovanna Rizzo,
Università degli Studi della Basilicata, Italy
Eirini Poulaki,
University of Texas at Austin, United States

*CORRESPONDENCE
Limei Tang,
tanglm@sio.org.cn

SPECIALTY SECTION
This article was submitted to Geochemistry, a section of the journal Frontiers in Earth Science

RECEIVED 10 June 2022
ACCEPTED 31 October 2022
PUBLISHED 12 January 2023

CITATION
Gao P, Tang L and Chen L (2023), Geochemistry and zircon U–Pb ages of early Ordovician syenites from the Inexpressible Island, Antarctica and tectonic implications.
Front. Earth Sci. 10:966085.
doi: 10.3389/feart.2022.966085

COPYRIGHT
© 2023 Gao, Tang and Chen. This is an open-access article distributed under the terms of the Creative Commons Attribution License (CC BY). The use, distribution or reproduction in other forums is permitted, provided the original author(s) and the copyright owner(s) are credited and that the original publication in this journal is cited, in accordance with accepted academic practice. No use, distribution or reproduction is permitted which does not comply with these terms.

Geochemistry and zircon U–Pb ages of early Ordovician syenites from the Inexpressible Island, Antarctica and tectonic implications

Peng Gao[1,2], Limei Tang[1,2]* and Ling Chen[1,2]

[1]Key Laboratory of Submarine Geosciences, Ministry of Natural Resources, Hangzhou, China, [2]Second Institute of Oceanography, Ministry of Natural Resources, Hangzhou, China

The Ross Orogenic Belt is in the Antarctica Transantarctic Mountains. North Victoria Land Granite Harbour Intrusive complex (GHI) records the tectonic-magmatism evolution of Ross orogeny. Extensively developed post-collisional granites around this margin of early Paleozoic magmatism can provide insights into the growth of continental crust through accretionary orogenesis. We provide geochemical and geochronological data from syenites from Terra Nova Bay, north Victoria Land in order to constrain its tectonic evolution and setting. The syenite belongs to the potassium-alkaline, calc-alkaline series and is characterized by high concentrations of rare Earth elements and large ion lithophile elements (LILE), and low content in high field strength elements (Nb, Ta, P, Ti). The petrographic and geochemical signatures show a possible island-arc granite affinity. LA-ICP-MS zircon U-Pb dating results suggest that the Inexpressible Island syenite was emplaced at ca. 471.8 ± 1.8 Ma and 477.3 ± 1.7 Ma, respectively. Zircon $\varepsilon_{Hf}(t)$ values range from −7.4 to −9.1; average −8.2 and whole-rock ε_{Nd} (t) values range from −8.5 to −10.3, indicating that formed by the partial melting of the lithospheric mantle enriched with subduction slab fluids and subcontinental lithosphere. Whereas, the syenite has a strong positive Eu anomaly and a positive Sr anomaly, suggesting that plagioclase cumulate crystallization occurred in the magma source area. Furthermore, through integration with previous studies, we suggest that syenite is a result of the melting zone of an older previously subduction enriched layer of the subcontinental lithospheric mantle (SCLM). To enable syenite emplacement we suggest a tectonic-magmatic model that invokes alternating phases of extension and contraction in the overriding plate. Finally, we report the youngest age of (post-orogenic) magmatism occurred during extension in the overriding plate ca. 478–471 Ma.

KEYWORDS

U-Pb geochronology, geochemistry, Rose orogeny, syenite, Inexpressible island

Introduction

Accretionary orogenesis is characterized by repeated cycles of subduction–accretion at interoceanic and continental convergent plate margins (Di Vincenzo and Rocchi, 1999; Condie, 2007; Li et al., 2016). The composition of accretionary orogenic belt complexes includes trench-arc-basin systems, seamounts, oceanic crust, and other relic geological records. It is also important for plate (especially micro-continental blocks) collision, assembly, and growth (Li et al., 2016) Repeated subduction–accretion cycles of rock units from continental and oceanic magmatic arcs, supra-subduction zone backarcs, and forearcs loaded with continent-derived materials form magmatic arcs. These magmatic igneous rocks record key information about the evolution of the subduction regimes of orogenic belts, such as subduction-dominating slab rollback and backarc opening, with mantle modifications occurring throughout. The origin of arc magmas involves multiple stages (Cawood et al., 2009; Rocchi et al., 2015), components, and processes, including, 1) the nature of the mantle source, 2) the activity and type of subduction components, and 3) the degree and depth of partial melting (Di Vincenzo and Rocchi, 1999; Rocchi et al., 2015). This variety of materials and processes makes orogenic igneous complexes a rich source of information. The identification of magmatic arcs in ancient accretionary orogens is thus important for understanding the structure and history of orogen genesis.

The Ross Orogen exposed in Victoria Land, Antarctica, is located at the Southern Ocean termination of the Transantarctic Mountains. It represents the along-strike continuation of the southeastern Australia margin prior to the Cretaceous breakup of Gondwana (Cawood, 2005; Cawood and Buchan, 2007; Paulsen et al., 2007; Elliot and Fanning, 2008; Vaughan and Pankhurst, 2008; Goodge, 2020). The Ross Orogen formed in the early Paleozoic within the framework of the convergence of the Paleo-Pacific oceanic plate and the Gondwana continental margin (Goodge, 2020). The Late Proterozoic to Early Paleozoic was characterized by widespread igneous activity in response to convergence along the Cambro-Ordovician margin of Gondwana (Cawood, 2005). In northern Victoria Land, Antarctica, large amounts of felsic to mafic plutonic rocks, known as the Granite Harbour Intrusive complex (GHI) (Gunn and Warren, 1962), were emplaced during the Cambro-Ordovician Ross Orogeny. In the coastal area of Terra Nova Bay, where Inexpressible Island is located, it is referred to as the Terra Nova Intrusive Complex (TeNIC) (Di Vincenzo and Rocchi, 1999), shows variable geochemical characteristics, suggesting the involvement of various distinct source rocks during the melting process (Di Vincenzo and Rocchi, 1999; Rocchi et al., 2015).

In the northern Victoria Land area, most of magma intrusive activity spanned ca. 545–485 Ma (Black and Sheraton, 1990; Tonarini and Rocchi, 1994; Rocchi et al., 1998; Fioretti et al., 2005; Tiepolo and Tribuzio, 2008; Hagen-Peter et al., 2015). Similar series of intrusion rocks in Australia which have the oldest age up to 514 Ma (Weis et al., 2006). In the central Transantarctic Mountains, calc-alkaline magmatism may have initiated as early as 590 Ma, and persisted for over 100 Ma (Goodge et al., 2012). As most of Antarctica is covered by ice and snow, it is difficult to know the age of the oldest magmatism. The age and geochemical patterns of intrusive rocks suggest oblique convergence along a tectonically segmented margin (Encarnación and Grunow, 1996; Rocchi et al., 1998; Goodge, 2002; Stump et al., 2003; Goodge et al., 2004; Goodge et al., 2012). The most recent magmatic processes formed the Vegetation Unit (~475 Ma), Abbott Unit (508 Ma), Irizar granite complex (~490 Ma) which have different source regions and intrusion depths but possess nearly identical rock compositions including granite, syenite, and lamprophyre (Borg et al., 1986; Borsi et al., 1995; Perugini et al., 2005; Chen et al., 2019). Research suggests that the Abbott Unit and Irizar complex was derived from partially melted mantle wedge above the subduction zone mixing with the continental lithospheric mantle, whereas the Vegetation Unit Lamprophyre was derived from partially melted ancient sub-continental lithospheric mantle mixing with crustal material under thinning lithosphere within the orogen (Di Vincenzo and Rocchi, 1999).

In this study, we conducted Sr-Nd isotope on two samples (N=2), major and trace element analysis of the whole rock (N=7), and zircon U-Pb dating as well as Hf isotopes ratios on two samples (N=2, n=40), from the early Ordovician syenite in the Inexpressible Island, northern Victoria Land, to further determine the nature, geochemical characteristics and petrogenesis of magmatism in the extensional environment of the late Ross orogeny.

Geological setting and sample characteristics

Convergence between the Antarctic part of Gondwana and the Paleo-Pacific oceanic lithosphere during the early Paleozoic (Dalziel, 1992) formed the Ross orogenic belt, which deformed and metamorphosed sedimentary rocks and granitic (sensu lato) plutons exposed along the Transantarctic Mountains (Borg and Depaolo, 1994; Stump, 1995) (Figure 1). The Proterozoic history and plate tectonic reconstruction of cratonic Antarctica as part of the Rodinia supercontinent are still a matter of debate (Moores, 1991; Dalziel, 1997; Fitzsimons, 2003; Pisarevsky et al., 2003). Northern Victoria Land lies at the Pacific termination of the Transantarctic Mountains. It is comprised of three different crustal blocks (Bradshaw and Laird, 1983) (Figure 1): 1) the Robertson Bay Terrane, with a Cambrian to early Ordovician thick flysch-type sequence (Kleinschmidt and Tessensohn, 1987; Stump, 1995; Rocchi et al., 1998; Bomparola et al., 2007); 2) the Bowers Terrane, a Cambrian complex of volcanic rocks and

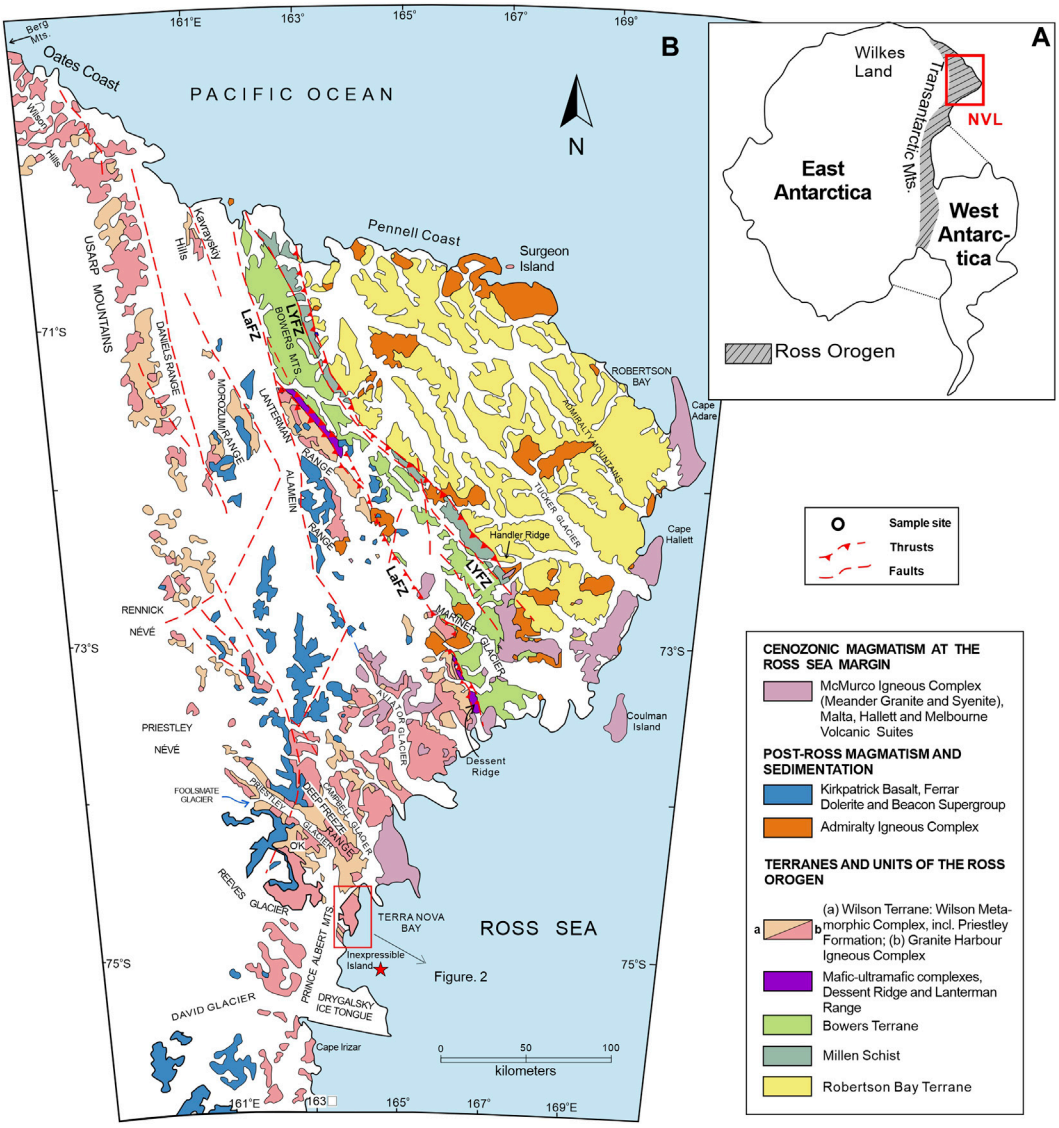

FIGURE 1
(A) The insert shows the location of the Ross Orogen and NVL (Boger, 2011; Rossetti et al., 2011; Fergusson et al., 2007). **(B)** Geological and tectonic sketch map of northern Victoria Land (NVL), Antarctica (modified after Estrada et al., 2016; Läufer et al., 2011; Di Vincenzo and Rocchi, 1999). LaFZ; Lanterman Fault Zone, LYFZ; Leap Year Fault Zone, O'K; O'Kane Canyon.

related sediments (Weaver et al., 1984; Crispini et al., 2007); and 3) the Wilson Terrane (Stump et al., 1983; Rossetti et al., 2006b; Di Vincenzo et al., 2014), a metasedimentary sequence including remnants of a polymetamorphic granulite complex (Castelli et al., 1991; Talarico and Castelli, 1995; Talarico et al., 1995) that experienced low-pressure low-to high-grade metamorphism during the Cambrian-Ordovician Ross Orogeny (Grew and Sandiford, 1984; Palmeri et al., 1994; Palmeri, 1997). An extensive association of mantle-derived calc-alkaline magmas and crustal melts that intruded the Wilson Terrane during the Ross Orogeny are collectively named the GHI (Gunn and Warren, 1962; Borg et al., 1987; Ghezzo et al., 1987; Kleinschmidt and Tessensohn, 1987; Vetter and Tessensohn, 1987; Armienti et al., 1990; Biagini et al., 1990; Stump, 1995; Di Vincenzo and Rocchi, 1999; Rocchi et al., 2004). Recent work (Fedrico et al., 2006; Bracciali et al., 2009; Rocchi et al., 2015, 2011) lead some models of tectonic evolution of the Ross Orogeny in the North Victoria Land (Rocchi et al., 2009; Rocchi et al., 2015). Studies show that the convergent margin of Gondwana land consists of a main continuous subduction zone coupled with local plate and transient subduction zones. These transient subduction zones are related to the continuous ribbons of outboard pieces of stretched forearc regions (Rocchi et al., 2011). The Ross Orogeny in Victoria Land was the result of

TABLE 1 Summary of syenites analyses project and mineral assemblage.

Sample name	Rock description		Location		Sr and Nd isotope ratio analysis	Photomicrographs	Bulk major and trace element analysis	Zircon cathodoluminescence (CL) images	U-Pb dating of zircon	In suit Hf isotope analysis	Mineral assemblage
			Lat	Long							
			(oS)	(oE)							
DJS-1	medium-to-coarse-grained with a granitic texture	Gray Bt syenite	−74.9194	163.6975	√	√	—	—	—	—	Q (25%) + Pl (25%) + Mc (20%) + *P*th (10%) + Bt (15%)
DJS-5a		Gray Bt syenite	−74.9194	163.6975	√	√	—	—	—	—	Q (35%) + Pl (15%) + Mc (25%) + *P*th (10%) + Bt (12%)
DJS-6		Gray syenite	−74.9194	163.6975	√	√	√	√	√	√	Q (35%) + Pl (12%) + Mc (25%) + *P*th (15%) + Bt (8%)
DJS-7		Gray Bt syenite	−74.9194	163.6975	√	√	—	—	—	—	Q (35%) + Pl (25%) + Mc (10%) + *P*th (10%) + Bt (15%)
DJS-13		Gray Hbl syenite	−74.9201	163.6943	√	√	√	√	√	√	Q (30%) + Pl (13%) + Mc (13%) + *P*th (25%) + Hbl (6%) + Bt (7%)
DJS-14		Gray Hbl syenite	−74.9201	163.6943	√	√	—	—	—	—	Q (30%) + Pl (17%) + Mc (13%) + *P*th (25%) + Hbl (6%) + Bt (7%)
DJS-15		Gray Hbl syenite	−74.9201	163.6943	√	√	—	—	—	—	Q (30%) + Pl (32%) + Mc (13%) + *P*th (12%) + Hbl (5%) + Bt (3%)

Note: Bt: biotite, Kfs: K-feldspar, Pl: plagioclase, Q: quartz; Mc: Microcline, *P*th: Perthite; Abbreviations of minerals based on Kretz (1983). Items that have been analyzed are indicated by "√", otherwise by "-"

10.3389/feart.2022.966085

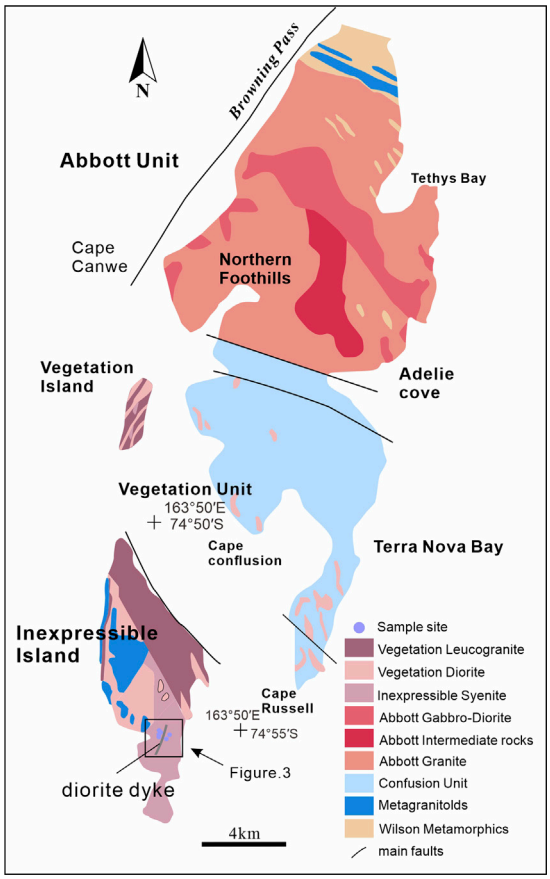

FIGURE 2
Geological and tectonic setting of the Inexpressible Island area showing the sample sites (Chen et al., 2019).

many stages of advancing and retreating subduction zone(s) (Rocchi et al., 2015, 2011). Thus, as an important part of the boundary between the Wilson arc and the forearc ribbon underwent subduction accretion and detachment, there is an abundance of magmatism in the North Victoria Land.

Syenite in the Inexpressible Island, Northern Victoria Land, is a confused and different part of the TeNIC unit, which is important to determining the nature, geochemical characteristics, and petrogenesis of magmatism in the extensional environment of the late Ross orogeny. We analyzed seven syenite samples (DJS-1, DJS-5a, DJS-6, DJS-7, DJS-13, DJS-14, and DJS-15) (see summary in Table 1) from the Inexpressible Island Dingjunshan area (Figure 2). A~ 5 m wide mafic dyke occurs with an approximately N-S trend and extends over 300 m across the syenite bedrock outcrop area (Figure 3A) (Chen et al., 2019). The syenite outcrops are composed of medium-to coarse-grained with gray-white color (Figures 3A–C), and samples were fresh and unweathered. The rock is mesocrystalline granitic structure and massive structure with a mineral assemblage of quartz 30%–35%, plagioclase 17%–25%, micro-plagioclase 10%–25%, Perthite 10%–25% and biotite 12%–15% (Figures 4D–I), and feldspars have experienced sericitization (Figure 4H). Some of syenite contain hornblende, which are associated with biotite, showing light green-brown green polychromatism (Figure 4H). The secondary mineral facies are mainly sericite and chlorite (Figure 4H), magnetite, zircon and apatite. Quartz ranges from euhedral and subhedral, sometimes can see anhedral crystal, and it can be seen that quartz and feldspar intergrow to form graphic texture (Figure 4H). The rock is a quartz syenite with a homogeneous isotropic texture (Figures 4D–I). A total of 7 samples are used in the study area.

Analytical methods

Zircon cathodoluminescence images

The internal structure of zircon can be revealed by the cathodoluminescence (CL) imaging technique. CL image can reflect the difference in the abundances of some trace elements (such as U, Y, Dy, and Tb) (Wu and Zheng, 2004), which can be influenced by temperatures at which the melts crystallized (Rubatto and Gebauer, 2000; Wu and Zheng, 2004; Rubatto and Gubauer, 2007), also the change of structural parameters such as crystallinity or the presence of defect centres can be reflected in CL image (Nasdala et al., 2002). The CL image can be used as a reference for tracing zircon origin. We have carried out CL photography on 40 zircon grains collected from two samples of DJS-6, DJS-13. Zircon CL images using an Analytical Scanning Electron Microscope (JSM-IT300) connected to a Delmic sparc system. The imaging condition was 0.5–30 kV voltage of electric field and 72 μA current of the tungsten filament.

U-Pb dating of zircon by LA-ICP-MS

40 zircon grains were collected using conventional density and magnetic separation techniques and picked out under a binocular microscope from two samples of DJS-6 and DJS-13, which finally have been used to do U-Pb dating. The grains were subsequently mounted in epoxy resin, polished to half their thickness and they were later photographed in transmitted and reflected light. We selected the location of the oscillatory-zoned rim or the location of the uniform color of cathode luminescence. And we avoided choosing cracks or inclusions area in the transmission-reflected image of zircon grains, the specified analysis spots are shown (Figure 5). U–Pb dating of zircon grains by LA-ICP-MS at the Wuhan SampleSolution Analytical Technology Co., Ltd., Wuhan, China. Detailed operating conditions for the laser ablation system and the ICP-MS instrument and data reduction are the same as described by Zong et al. (2017). Laser sampling was performed using a GeolasPro laser ablation system that consists of a COMPexPro 102 ArF excimer laser (wavelength of 193 nm and maximum energy

FIGURE 3
Representative outcrops and photomicrographs of granites from Inexpressible Island, NVL. **(A)** The field contact relationship between diorite and syenite is shown in the figure, which shows diorite dyke. **(B)** Massive syenite occurs in the field. **(C)** Syenite bedrock in the eastern bay region.

of 200 mJ) and a MicroLas optical system. An Agilent 7900 ICP-MS instrument was used to acquire ion-signal intensities. Helium was applied as a carrier gas. Argon was used as the make-up gas and mixed with the carrier gas *via* a T-connector before entering the ICP. A "wire" signal smoothing device is included in this laser ablation system (Hu et al., 2015). The laser beam spot and frequency of the GeolasPro for this analysis were 32 μm and 5 Hz, respectively. Zircon isotope ratios were calibrated by standard sample Plešovice 338.15 ± 1.7 Ma (Sláma et al., 2008), and isotope ratio monitoring standard sample GJ-1,599.0 ± 1.7 Ma (Jackson et al., 2004). All time-resolved analysis data consisted of approximately 20–30 s of blank signal and 50 s of sample signal. Offline processing of the analytical data (including the selection of sample and blank signals, instrument sensitivity drift correction, and U-Pb isotope ratio and age calculation) was undertaken using the software ICPMSDataCal (Liu et al., 2008, 2010). U-Pb age harmonic mapping and age-weighted average calculations of zircon samples were carried out using Isoplot/Ex_ver3 (Ludwig, 2003).

Whole rock major element analysis

We have analyzed the content of major elements in seven syenite samples (DJS-1, DJS-5a, DJS-6, DJS-7, DJS-13, DJS-14, DJS-15) from the Inexpressible Island. Major element analyses of whole rock were conducted on XRF (Primus II, Rigaku, Japan) at the Wuhan Sample solution Analytical Technology Co., Ltd., Wuhan, China. The detailed sample-digesting procedure was as follows: 1) Sample powder (200 mesh) was placed in an oven at 105°C for drying of 12 h; 2) ~1.0gdried sample was accurately weighted and placed in the ceramic crucible and then heated in a muffle furnace at 1000°C for 2 h. After cooling to 400 °C, this sample was placed in the drying vessel and weighed again in order to calculate the loss on ignition (LOI). 3) 0.6 g sample powder was mixed with 6.0 g cosolvent ($Li_2B_4O_7$: $LiBO_2$: LiF = 9: 2:1) and 0.3 g oxidant (NH_4NO_3) in a Pt crucible, which was placed in the furnace at 1,150°C for 14 min. Then, this melting sample was quenched with air for 1 min to produce flat discs on the fire brick for the XRF analyses.

Whole rock trace element analysis

We have analyzed the content of trace and rare Earth elements in seven syenite samples (DJS-1, DJS-5a, DJS-6, DJS-7, DJS-13, DJS-14, DJS-15) from the Inexpressible Island. Whole-rock trace and rare Earth elements were analyzed by ICP-MS (Agilent 7700e). The detailed sample-digesting procedure was as

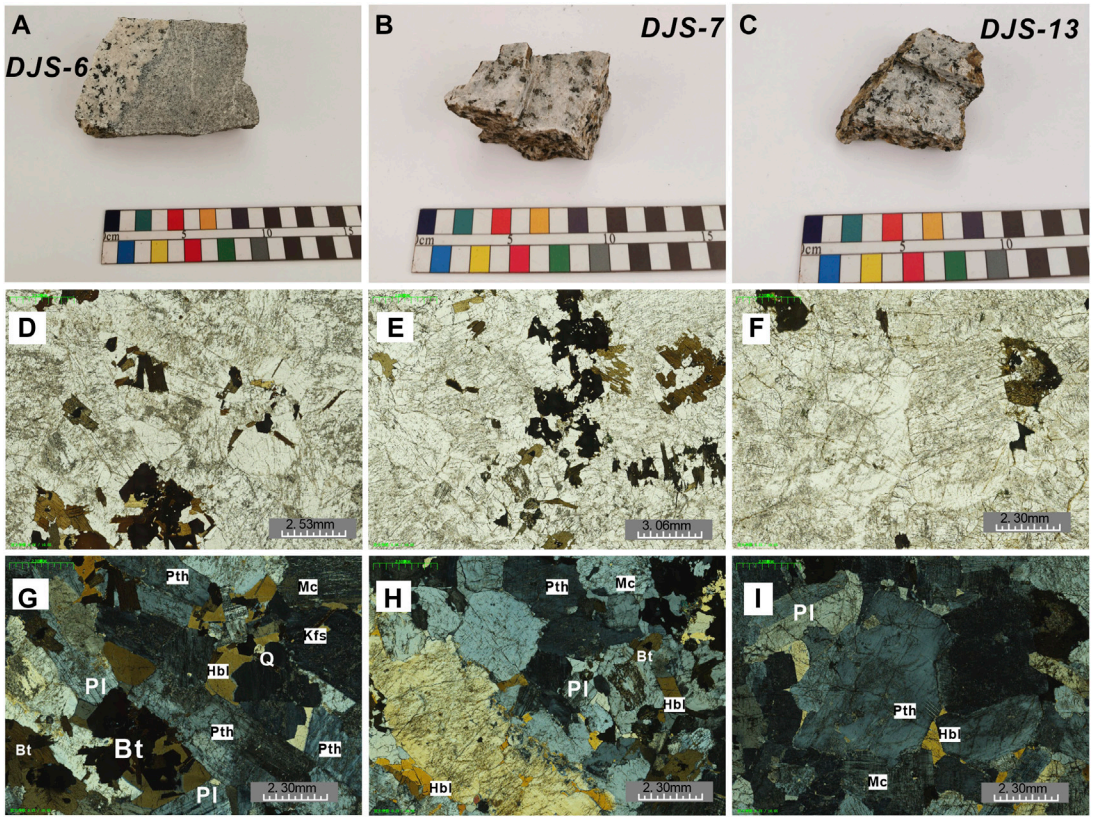

FIGURE 4
Representative photomicrographs of Early Ordovician syenite from Inexpressible Island. **(A)**, **(B)** and **(C)** Photographs of the syenite. **(D)**–**(I)** polarizing microscope and Cross polarized light photomicrograph. Bt: biotite, Kfs: K-feldspar, Pl: plagioclase, Q: quartz; Mc: Microcline, Pth: Perthite.

follows: 1) Sample powder (200 mesh) was placed in an oven at 105°C for drying of 12 h; 2) 50 mg sample powder was accurately weighed and placed in a Teflon bomb; 3) 1 ml HNO_3 and 1 ml HF were slowly added into the Teflon bomb; 4) Teflon bomb was put in a stainless-steel pressure jacket and heated to 190°C in an oven for >24 h; 5) After cooling, the Teflon bomb was opened and placed on a hotplate at 140°C and evaporated to incipient dryness, and then 1 ml HNO_3 was added and evaporated to dryness again; 6) 1 ml of HNO_3, 1 ml of MQ water and 1 ml internal standard solution of 1ppm In were added, and the Teflon bomb was resealed and placed in the oven at 190°C for >12 h; 7) The final solution was transferred to a polyethylene bottle and diluted to 100 g by the addition of 2% HNO_3.

Zircon *in situ* Hf isotope analysis of zircon by LA-MC-ICP-MS

We choose to conduct Hf analysis in a place where the surface is relatively uniform or close to the U-Pb analysis spots, in order to obtain fairly accurate Hf isotope ratios, these analytical spots are as shown (Figure 5). 40 zircon grains collected from two samples of DJS-6 and DJS-13 have been used to do *in situ* Hf dating. Experiments using *in situ* Hf isotope ratio analysis were conducted using MC-ICP-MS in combination with an excimer ArF laser ablation system hosted at Wuhan Sample Solution Analytical Technology Co., Ltd. All data were acquired on zircon in single spot ablation mode at a spot size of 44 μm. The energy density of the laser ablation used in this study was ~8.0 J cm^{-2}. Each measurement consisted of 20 s of acquisition of the background signal followed by 50 s of ablation signal acquisition. The operating conditions for the laser ablation system and the MC-ICP-MS instrument and analytical method were the same as described (Hu et al., 2012). To ensure the reliability of the analysis data, three international zircon standards of 91500 $^{176}Hf/^{177}Hf$= 0.282308, (Zhang and Hu, 2020), and GJ-1 $^{176}Hf/^{177}Hf$= 0.282013, (Zhang and Hu, 2020), were analyzed simultaneously with the samples. GJ-1 was used as the second standards to monitor the quality of the data correction. The external precision (2SD) of 91,500 and GJ-

FIGURE 5
Representative cathodoluminescence images of zircons from the dated samples from Inexpressible Island showing U-Pb ages and the location of the analyzed Hf.

1 was better than 0.000020. The Hf isotopic compositions of 91,500 and GJ-1 have been reported (Zhang and Hu, 2020).

Sr and Nd isotope ratio analysis by LA-ICP-MS

We analyzed the content of Sr and Nd isotope ratios in two syenite samples (DJS-6, DJS-13) from the Inexpressible Island. Sr and Nd isotope analyses were performed on an MC-ICP-MS at the Wuhan Sample Solution Analytical Technology Co. Analyses of the NBS 987standard solution yielded $^{87}Sr/^{86}Sr$ratio of 0.710244 ± 22 (2SD, n=32, Thirlwall M. F, 1991), which is identical within error to their published values (0.710241 ± 12, Thirlwall, 1991). All data reduction for the MC-ICP-MS analysis of the Sr isotope ratios was conducted using Iso-Compass software (Zhang et al., 2020). The USGS reference materials BCR-2 (basalt) and RGM-2 (rhyolite)yielded results of 0.705034 ± 14 (2SD, n=4) and 0.704192 ± 10 (2SD, n=4) for $^{87}Sr/^{86}Sr$, respectively, which is identical within error to their published values (Li et al., 2012). In addition, One JNdi-1standard was measured for every ten samples analyzed in Nd isotopes analysis. Analyses of the JNdi-1standard yielded $^{143}Nd/^{144}Nd$ratio of 0.512118 ± 15 (2SD, n=31), which is identical within error to their published values (0.512115 ± 07, Tanaka et al., 2000).

Results

Zircon U-Pb geochronology

In this study, LA-ICP-MS zircon U-Pb dating analysis was performed on syenite samples DJS-6 and DJS-13 from the TeNIC. The results are shown in (Supplementary Table SA1) and Figure 6. All spots on the oscillatory-zoned rim domains of zircon grains from the samples tightly cluster or are close to the Concordia line, all data Concordia filter better than 95% in error ellipses. The integration time is set to 30–35s according to the

recommended value of the monitoring standard sample. We allow for an age error of better than 1% (See Supplementary Table SA1). Most zircons from the syenite samples of DJS-6 and DJS-13 were dominantly euhedral to subhedral. The CL images display reduced CL contrast between bands which are sometimes broad, also sometimes appear as sector zoning, were generally 100–180 μm and 80–100 μm in size, and had length/width ratios of 1:1–3:1 and 1:1–2:1, respectively (Figure 5). In total, 40 grains were analyzed from sample DJS-6 and DJS-13, yielded Th/U ratios of 0.58–0.78 and 0.46–0.83, respectively (Supplementary Table SA1). The concordia ages of DJS-6 is 471.8 ± 1.8 Ma (2σ, MSWD = 0.87, Probability = 0.35, *n*=20) (Figure 6A), giving a weighted mean $^{206}Pb/^{238}U$ age of 471.8 ± 3.5 Ma (2σ, MSWD = 0.87; *n*=20) (Figure 6B). The concordia ages of DJS-13 is 477.3 ±1.7 Ma (2σ, MSWD = 0.59, Probability = 0.44, *n*=20) (Figure 6C). $^{206}Pb/^{238}U$ age of 477.3 ± 3.4 Ma (2σ, MSWD = 0.59; *n*=20) (Figure 6D).

Whole rock geochemistry

The whole-rock geochemical compositions of the syenite unit are listed in (Supplementary Table SA2). The rocks yielded concentrations of 60.88–62.81 wt% SiO_2 with 10.02–11.72 wt% total alkalis. The K_2O/Na_2O ratios varied from 0.34 to 0.39 (Supplementary Table SA2). The Inexpressible Island high-potassium syenite shows different evolutionary paths (Figures 7A,B). All the samples are plotted in the shoshonite series field on the K_2O vs. SiO_2 diagram (Figure 7C). Our samples contain low MgO (0.36–0.53 wt%), TiO_2 (0.43–0.66 wt%), and P_2O_5 (0.11–0.18 wt%) contents with a relatively high Al_2O_3 (17.46–18.46 wt%), the $Al_2O_3/(CaO + Na_2O + K_2O)$ (A/CNK) in molar proportion values ranging from 0.94 to 1.08, indicating that metaluminous to peraluminous (Figure 7B). Chondrite-normalized rare Earth elements (REE) concentrations of the syenite are shown in (Figure 8A) (Sun and McDonough, 1989). The ΣREE

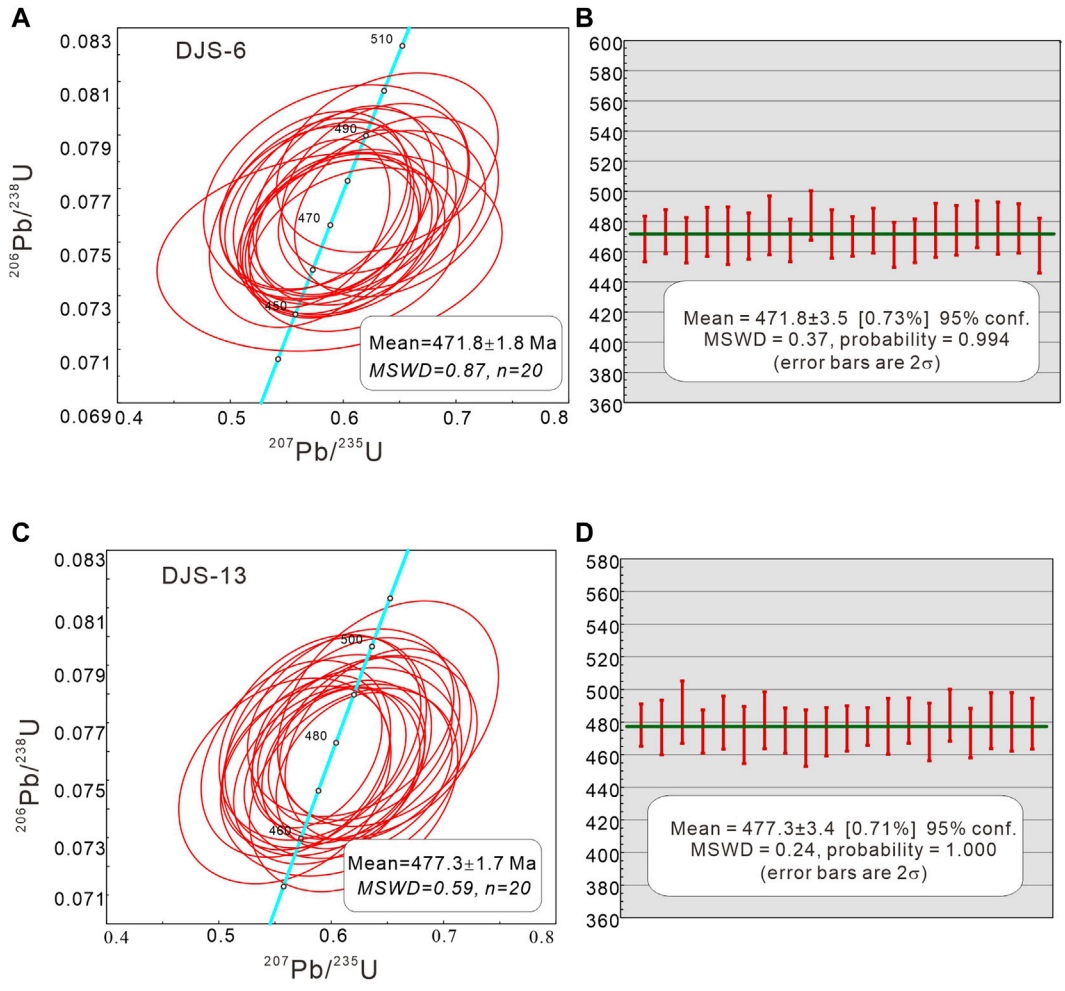

FIGURE 6
Zircon U–Pb concordia diagrams **(A,C)**, weighted mean $^{206}Pb/^{238}U$ ages **(B,D)** of the Inexpressible Island syenites, northern Victoria Land.

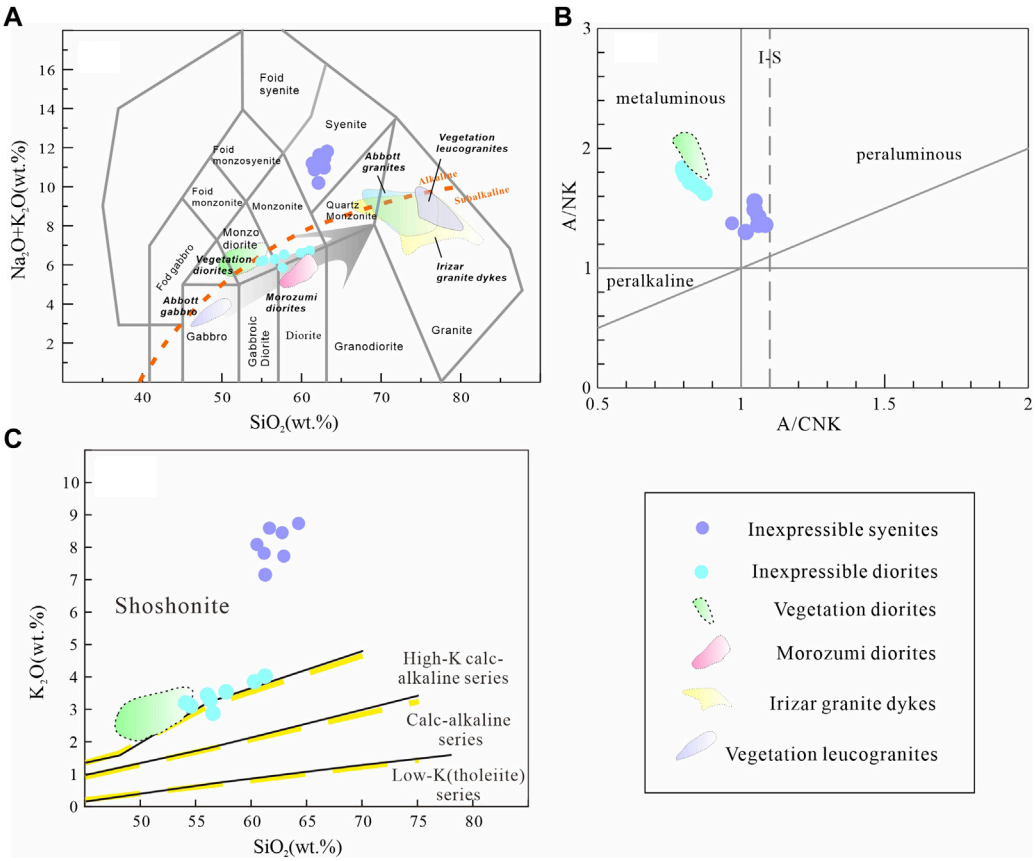

FIGURE 7
(A) Total alkali-silica diagram for the Inexpressible Island syenite (Middlemost, 1994), **(B)** A/NK vs. A/CNK modifications (Maniar and Piccoli, 1989). and **(C)** K_2O vs. SiO_2 diagram (Peccerillo and Taylor, 1976), Inexpressible Island syenite compared to the Inexpressible Island diorite dyke (Chen et al., 2019; Gao et al., 2022), Vegetation Island diorites (Rocchi et al., 2009) and Irizar dyke, and Morozumi diorite samples (Rocchi et al., 2015).

concentrations displayed negative trend than diorites, and strongly enriched Eu anomalies (0.89–5.58) (Supplementary Table SA3). On the primitive mantle-normalized multi element diagram, the syenite showed negative Th (1.60–5.78 ppm), P (4.82–8.31 ppm), and Ti (1.98–3.02 ppm) anomalies and positive Rb (134.8–269.4 ppm), Ba (3,368–5,003 ppm), Pb (14.31–34.89 ppm), K (241.0–289.2 ppm), and Zr (92.6–465.9 ppm) anomalies than the Inexpressible Island diorites (Figure 8B).

Whole-rock Sr-Nd isotopes

Whole-rock Sr-Nd isotope data for the Inexpressible medium- and coarse-grained syenites are listed in Supplementary Table SA4. Whole-rock $(^{87}Sr/^{86}Sr)_i$ and $\varepsilon_{Nd}(t)$ values were calculated as 471.8 Ma for DJS-6 and 477.3 Ma for DJS-13. The Inexpressible syenites had similar $\varepsilon_{Nd}(t)$ values, ranging from −8.5 to −10.3, and a high and narrow range of initial $^{87}Sr/^{86}Sr$ values, ranging from 0.7104 to 0.7128.

Zircon Lu-Hf isotopes

The zircons used for the U-Pb dating were used for the *in situ* or counterpoint zircon Hf isotope analyses (Supplementary Table SA5). The initial $^{176}Hf/^{177}Hf$ ratios for the zircons from the DJS-13 syenite with Early Ordovician ages ranged from 0.282228 to 0.282276. Their $\varepsilon_{Hf}(t)$ ranged from −7.4 to −9.1 (Figure 9). (Supplementary Table SA5). The $\varepsilon_{Hf}(t)$ values for the zircons from the DJS-6 syenite ranged from −7.4 to −9.0.

Discussion

Timing of the magmatism

Previous published chronological studies of the Terra Nova igneous body suggest the extensive Rose Orogeny magmatism, such as, calc-alkaline granites in the eastern Mountaineers Range

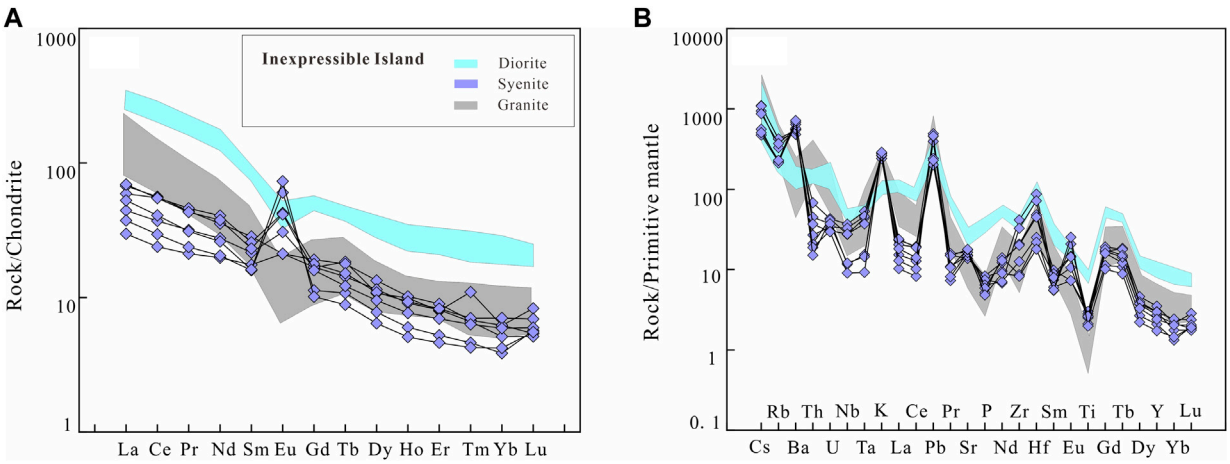

FIGURE 8
Primitive mantle-normalized plots of incompatible elements and chondrite-normalization plots (Sun and McDonough, 1989) of trace elements, trace element data from the diorite and granite are from Gao et al. (2022) and Chen et al. (2019), respectively.

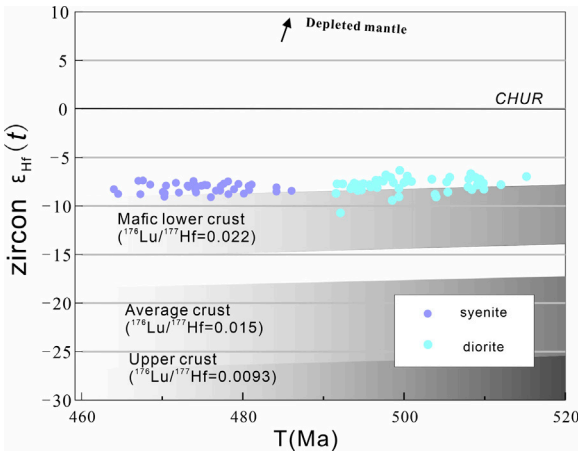

FIGURE 9
Zircon $\varepsilon_{Hf}(t)$ vs. T (Ma) plot of the Inexpressible Island syenite and diorite (Gao et al., 2022).

by Rb-Sr pseudo-isochron dating are 610 Ma ages (Bomparola et al., 2007); The granodiorite of the Wilson terrane zircon shows U-Pb ages of 496.7 ± 6.8 Ma (Rocchi et al., 2015); The U-Pb ages of quartz diorite and tonalite intrusions of the granitic mafic body in the Vegetation Island zircon are ranging from 521 Ma to 487 Ma (Rocchi et al., 2004); Zircon U-Pb age of tonalites from the Inexpressible Island is 482 ± 4.2 Ma (Wang et al., 2014). In this study, zircon U-Pb dating (Supplementary Table SA1) of the medium- and coarse-grain potassic syenite (DJS-6) and the medium-grain potassic syenite (DJS-13) from Inexpressible Island yielded crystallization ages of 471.8 ± 1.8 Ma and 477.3 ± 1.7 Ma, respectively, (Figures 6A,B). These results suggest that the syenites were emplaced in the early Ordovician. Based on the age variation of intrusions, an extensive and long-lasting multi-episode magmatism was active at the Wilson Terrane continental margin (Borg et al., 1986; Borsi et al., 1995; Perugini et al., 2005; Rocchi et al., 2004; Chen et al., 2019; Goodge, 2020; Gao et al., 2022). In addition, it shows slightly different core-mantle relationships in different zircon grains of the same massive syenite rock in CL images. Most grains have gray-dark cores and bright mantles, with high Th/U ratios (Supplementary Table SA1). And some zircon grains display reduced CL contrast between bands in CL images which are sometimes broad, and also sometimes appear as sector zoning, yielding Th/U ratios of 0.46–0.83, with average Th/U >0.5 (Figure 5 and Supplementary Table SA1). Generally,

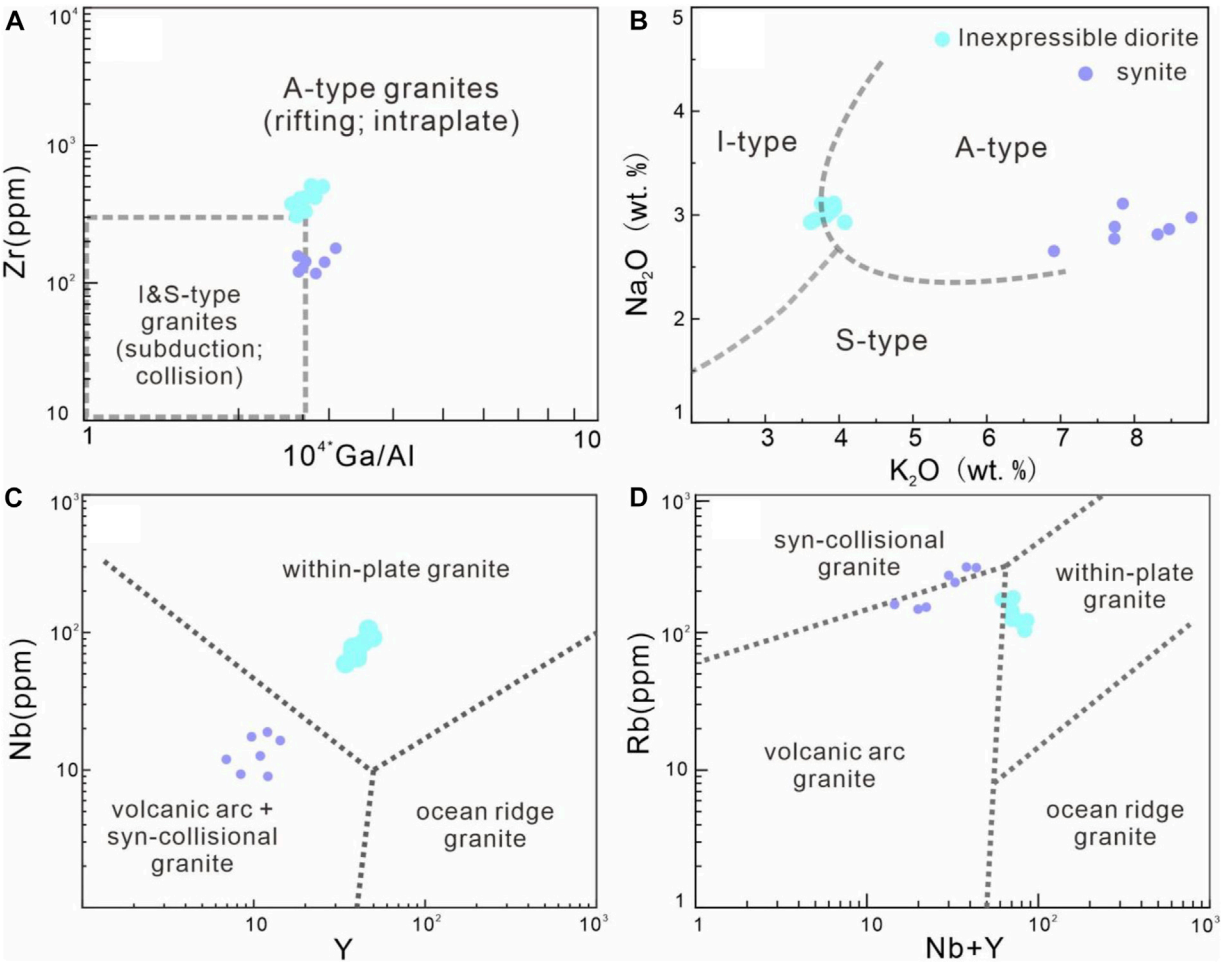

FIGURE 10
Structural environment diagram of the rocks in the Inexpressible Island intrusive. **(A)** 10^4*Ga/Al vs. Zr diagram (Whalen et al., 1987); **(B)** K_2O vs. Na_2O; **(C)** and **(D)** Nb vs. Y and Rb vs. Nb+Y diagrams (Pearce et al., 1984).

the Th/U of magmatic zircon is greater than 0.1 (Hoskin and Schaltegger, 2003). Combined with CL image and Th/U content characteristics, we suggest that zircons of the Inexpressible Island syenites belong to magmatic origin. Bomparola et al. (2007) point out the presence of long-term shallow crustal magmatism in the north Victoria land. They suggest that extensive and long-term extensional processes occurred during the Ross Orogeny as early as 530 Ma, which indicates prolonged thermal anomalous thermal activity beneath this region (Bomparola et al., 2007). We suggest that long-period magmatic events extended to ca. 470 Ma. Further, in the tectonic discrimination diagrams of 10^4Ga/Al vs. Zr, K_2O vs. Na_2O, Y vs. Nb, and Nb+Y vs. Rb (Figures 10A–D), all the syenite samples belong to either A-type granite and syncollisional or volcanic arc granite and represent post-orogenic granitoids (Pearce et al., 1984). A-type granitoids are generally emplaced in an extensional environment: post-collisional or anorogenic (Whalen et al., 1987; Eby, 1992, 1990; Wu et al., 2002; Bonin, 2007). Although, it is possible for the magma geochemistry to vary independently of the tectonic setting (Volkert et al., 2000; Jacobs and Thomas, 2004; Köksal et al., 2004; Whalen et al., 2006). But the Inexpressible Island syenites are associated with magmatic activity in widespread tectonic extension (Rocchi et al., 2004; Bomparola et al., 2007).

Petrogenesis

The mineralogical and chemical composition of the syenites associated with the Inexpressible Island area, comprising of alkaline-feldspar and perthite, coupled with high content of high field strength elements such as Zr, Hf, slightly decrease in their ΣREE content (expect for Eu) (Figures 8A,B), when compared to S-type and I-type granitoid suggest that the granitoid are typically syenite and A-type (e.g., Eby, 1992).

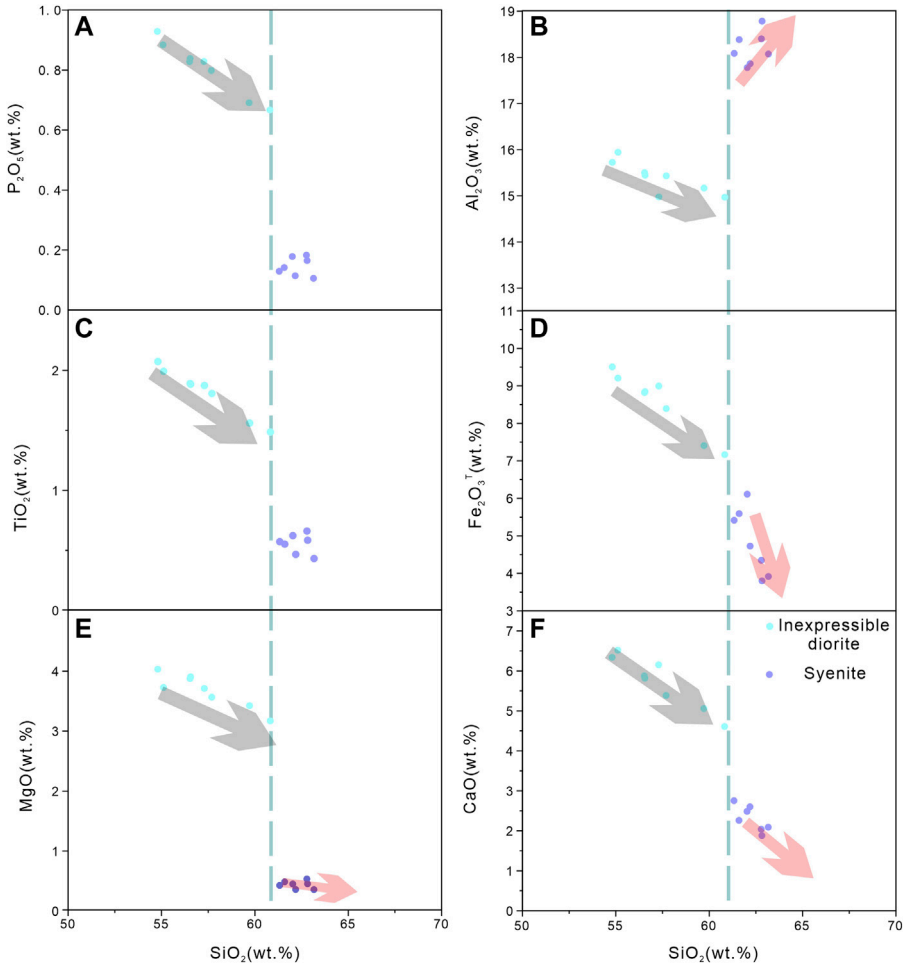

FIGURE 11
Harker diagrams for the medium- and coarse-grained syenites. Diorite data are derived from Gao et al., 2022. The dashed blue line indicates distinct chemical gaps.

Similarly, these syenites are equivalent to TeNIC post-collisional granitoids complex is also have common content of HFSE and LILE, also low content of Ti, P, Nb, Ta, Th, and ΣREE. region monzogranites, diorites, and granites were all in the calc-alkaline series (Rocchi et al., 2009) (Figure 7C). Whole-rock geochemistry from the Inexpressible Island syenite indicates weakly peraluminous to metaluminous with high potassium-alkaline content (Figure 7B). The average K_2O/Na_2O was 2.77, and on a SiO_2 vs. K_2O diagram (Figure 7C), the samples fall in the shoshonite region, indicating a highly potassium-rich source. Among the mafic igneous rocks from the early Paleozoic Ross Orogen of northern Victoria Land, the Morozumi diorite displayed a strong affinity to potassic rocks, such as the Vegetation Island lamprophyres, representing mantle-derived magmas emplaced during the late orogenic to post-collisional stage (Di Vincenzo and Rocchi, 1999; Rocchi et al., 2009). Whole rocks of the Inexpressible Island syenites have a very high total alkali content, which is over than the evolution trend of other TeNIC (Terra Nova intrusive complex) rock masses in the TAS diagram (gray arrow in the figure) (Figure 7A). The Harker diagrams and REE distribution patterns suggest that fractional crystallization played an important role in the differentiation of the syenite rocks. More specifically, the decrease of MgO, $Fe_2O_3^T$ (Figures 11D,E), with SiO_2 indicates the fractional crystallization of clinopyroxene and hornblende. The decrease of $Fe_2O_3^T$ also indicates the fractional crystallization of magnetite. The decrease of CaO and Sr with SiO_2 in the syenites is consistent with cumulus crystal of plagioclase while the decrease of Ba, and the strong positive Eu anomaly, are consistent with cumulus crystal of plagioclase. This is also in accordance with petrographic observations. Elements Nb, Ta and Ti are usually used to differentiate the rocks' formation as well as in tracing contamination of mantle derived *via* crustal assimilation (e.g., Niu and O' Hara, 2009; Wang et al., 2017). This came from the

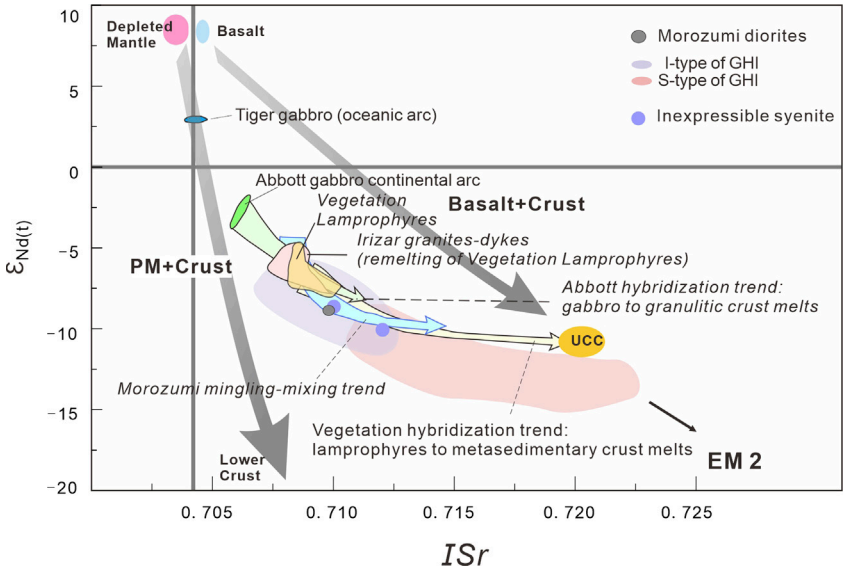

FIGURE 12
$\varepsilon_{Nd}(t)$ vs $(^{87}Sr/^{86}Sr)_i$ plot of the Inexpressible Island intrusive rocks. Also reported for comparison are 1) intrusive complexes emplaced around 490–500 Ma in the Wilson arc; 2) Abbott gabbro and its hybridization from deep-crust melts, Vegetation Island leucogranites and their hybridization from metasedimentary upper-crust melts (Di Vincenzo and Rocchi, 1999; Rocchi et al., 2004); 3) Irizar granites and dykes (Rocchi et al., 2009); 4) intrusive rocks emplaced earlier in the Tiger oceanic arc, that is, the Tiger gabbro (Bracciali et al., 2009); 5) intrusive rocks of the Morozumi mafic-intermediate (Rocchi et al., 2015); and 6) I-type and S-type Granites Harbour Intrusive (Armienti et al., 1990). Modifications (Jahn, et al., 1999; Rocchi et al., 2015). The gray arrow shows a simple mixing-milling trend for source and melts contaminations. The mixing parameters used are referred to. UM denotes upper mantle peridotites, UCC, upper continental crust elemental data (Taylor and McLennan, 1985), MCC-LCC, middle to lower crust data of middle crust (Rudnick and Fountain, 1995).

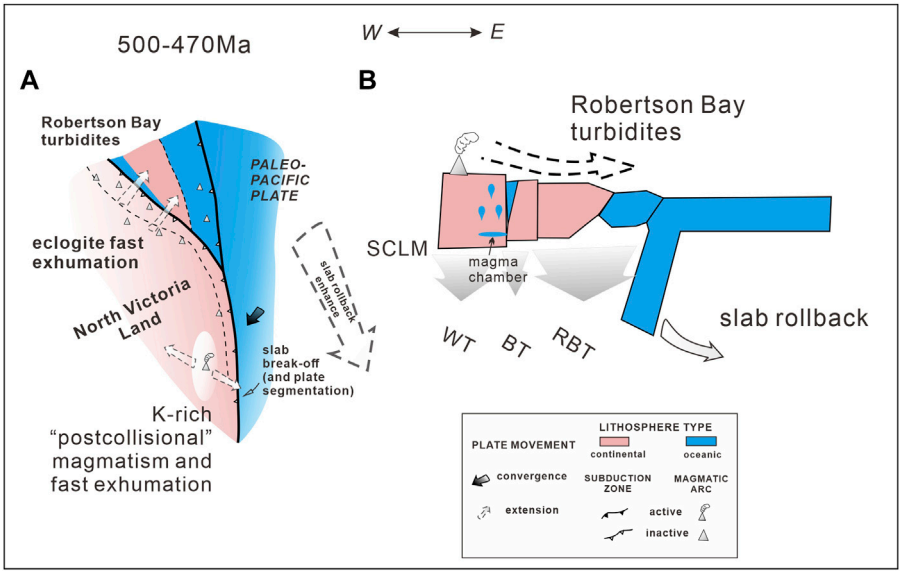

FIGURE 13
Regional tectonic schematic cartoon after **(A)** Late Ross orogenic stage post-collisional potassic magmatism. **(B)** Schematic diagram of subduction zone structure. Modifications after reference (Goodge, 2002; Rocchi et al., 2009; Rocchi et al., 2011).

fact that rocks that formed from melting of crustal material generally showed significant depletion in Nb, Ta, and Ti when compared to rocks that formed from mantle derived magmas (e.g., Niu and O' Hara, 2009'; HaraStanley, 1984; Rudnick and Gao, 2003; Taylor and McLennan, 1985; Taylor, 1977). This suggests a genetic link between the formation of continental crust and subduction related (island arc) magmatism (Taylor, 1977; Taylor and McLennan, 1985). The obviously negative Nb and Ta anomalies in cal-alkaline syenites from the Inexpressible Island is therefore consistent with rocks derived from melting of crustal sources. And also, the geochemical characteristics of the syenites such as their high K_2O and Na_2O and low Y/Nb ratio<2 are commonly considered as derivatives of enriched OIB mantle sources (Eby, 1992, 1990; Bonin, 2007). Otherwise, ratios of some LILE and HFSE such as Th/Ta, Th/Nb, Rb/Nb, Ba/Nb generally reflect the source materials from which igneous rock was derived (e.g., Shellnutt et al., 2009). This is because these trace elements remain largely immobile throughout the course of magmatic differentiation (Shellnutt and Zhou, 2007; Shellnutt et al., 2009; Wang et al., 2017). Typically, mantle derived rocks generally have lower Th/Ta ratio≈2 compared to the upper crust (Th/Ta≈6.9) or lower crust (Th/Ta≈7.9) (Rudnick and Gao, 2003; Shellnutt et al., 2009). The average Th/Ta values obtained from the samples of syenites are approximately 2, the ratio of individual is up to 9.5, which further suggests that the syenites were most likely derived from the mantle. The syenite is characterized by high $(^{87}Sr/^{86}Sr)_i$ values (0.7033–0.7045) and low $\varepsilon_{Nd}(t)$ values (Figure 12 and Supplementary Table SA4), which exhibit evolutionary isotopic characteristics to initial melts simulated by a previous study on TeNIC rocks, indicate syenite of the Inexpressible Island are hybridization from metasedimentary upper-crust and mantle melts (Di Vincenzo and Rocchi, 1999; Rocchi et al., 2015). The $\varepsilon_{Hf}(t)$ values of the oscillatory magmatic zircon rims show a range from −7.4 to −9.1 (Figure 9), suggesting that the occurrence of Mesoproterozoic crust and both reworked ancient crustal (Condie et al., 2005; Wu et al., 2006; Zheng et al., 2007). In addition, trace element geochemical signatures of the syenite show significant enrichment (Sr, Zr and Eu) than granites (Figure 8B), and similar to diorite (Chen et al., 2019), it suggests that the syenite magmas associated with these previous diorites. No coeval mafic-ultramafic rocks have been found in the Inexpressible Island, so as Morozumi diorite and Vegetation lamprophyre, are considered to be enriched by enrich mantle melting (Rocchi et al., 2009; Rocchi et al., 2015). However, compared with the spatially proximal diorite, trace element composition is more depleted (Figure 8A). Considering the significant differences in the evolution of major and trace elements, we believe that the lithospheric mantle beneath the Wilson continental margin is heterogeneous or represents a more complex compositional evolution.

Rocchi et al. (2015) established a genetic link between mafic, diorite, and granite of GHI in the northern Victoria Land *via* a liquid line of decent involving fractional crystallization and/or assimilation fractional crystallization (AFC) of enrich mantle derived magmas. Parabolic trends of the Granite Harbour intrusive samples suggest mixing between old crust with low $\varepsilon_{Nd}(t)$ and high $(^{87}Sr/^{86}Sr)_i$ and a juvenile component with higher $\varepsilon_{Nd}(t)$ and low $(^{87}Sr/^{86}Sr)_i$ (Figure 12). These results are consistent with the interpretation of Rocchi et al. (2009), who suggested that the late-stage diorite with low $\varepsilon_{Nd}(t)$ in northern Victoria Land was sourced from enriched subcontinental lithospheric mantle. In addition, Hagen-Peter et al. (2015) suggest that low Subcontinental lithospheric mantle Hf values may be in response which may be due to metasomatism of subduction materials that occurred during the late Ross orogeny, including fluid metasomatism, subduction of pelagic sediments, and introduction of crust-derived materials by subduction erosion.

The definition of "ultrapotassic rocks" introduced by (Foley et al., 1987) is based on their whole-rock chemistry rather than mineralogy. Commonly, all of these tectonic settings, except for intra-plate settings, are related to subduction zones. Several models have been proposed to explain the origin of ultrapotassic rocks, all of which invoke low degrees of melting of a metasomatized upper mantle. Experimental work has demonstrated that peridotite melts which formed in the presence of CO_2 at pressures ~27 kbar would be carbonatitic, whereas the presence of H_2O or F may enhance the stability of phlogopite (Eggler, 1978; Wendlandt, 1984). These studies suggest that small degrees of partial melting of phlogopite-bearing peridotite at depths below the level of amphibole stability and in the presence of CO_2 produces a high K_2O liquid with high Mg/Ca. All of these metasomatic processes and often associated with either intraplate rifting or subduction (Nelson et al., 1986). Extensive geochemical analysis (N100 samples) and zircon U–Pb geochronology (n = 70) confirm that alkaline and carbonatitic magmatism was partially contemporaneous with the emplacement of large subduction-related igneous complexes in adjacent areas. The SCLM has frequently been invoked as a potential source of alkaline silicate rocks and associated carbonatites in many localities (Bailey, 1987; Serri et al., 1993; Arzamastsev et al., 2001; Downes et al., 2005). The ultra-potassium syenite of the Inexpressible Island has a positive Eu anomaly (From 0.8 to 5.58) and is enriched in Sr (Figures 8A,B), which is indicative of that plagioclase cumulate crystallization occurred in the magma chamber. Experimental petrology shows that phlogopite has higher Rb/Sr and lower Ba/Rb values in the residual phase during partial melting, while hornblende shows the opposite (Furman and Graham, 1999). The Rb/Sr (0.36–0.92; mean 0.61) and Ba/Rb ratios (12.63–35.35; average 23.44) in the syenite samples shown considerable variation (Supplementary Table SA3). We suggest that the variation in Rb/Sr and Ba/Rb ratios reflect the complex genesis of the magma source, which may have been jointly controlled by phlogopite and hornblende.

Tectonic implications

Early Paleozoic convergence between the East Antarctic Craton and the Paleo-Pacific oceanic plate gave rise to southwest-directed

subduction (present-day coordinates) and related continental and oceanic arc magmatism (Weaver et al., 1984; Borg et al., 1986; Kleinschmidt and Tessensohn, 1987; Dalziel, 1997; Rocchi et al., 1998). The ongoing convergence eventually led to the formation of the Ross Orogen (Stump, 1995), as a result of accretion on the Antarctic margin of variable crustal blocks, although this is still a matter of debate (Weaver et al., 1984; Finn et al., 1999; Federico et al., 2006). A synthesis of recent research suggests that the final northern Victoria Land juxtaposition occurred during the Early Paleozoic and was accompanied by extensive post-collisional extensional magmatism (Goodge, 2020; Rocchi et al., 2015; Federico et al., 2009). At this time, the edge of the subduction zone was being obliquely subducted along the Ross orogenic belt toward northern Victoria Land (Janosy and Wilson, 1995) alkaline magmatism is interpreted to be a result of either crust-mantle interactions or a mantle plume in the shallow part of the crust due to intra-plate rifting or post-orogenic extensional tectonics (Wilson et al., 1995; Yang et al., 2012). Lithosphere delamination (Bird, 1979; Liégeois and Black, 1987) convective removal of the lithosphere (Houseman et al., 1981), and slab breakoff (Liégeois and Black, 1987; Davies and Von Blankenburg, 1995) have been proposed to explain magmatism in post-collisional and post-orogenic settings, also are used to make an explanation of the tectonic setting of the Ordovician granitic magmatism in the Wilson terrane (Rocchi et al., 2015; Hagen-Peter and Cottle, 2016), These processes induce an upwelling of the asthenosphere, which in turn, induces melting of the subcontinental mantle lithosphere (Wilson et al., 1995; Yang et al., 2012). Previous studies have shown that the typical post-collisional magmatic assemblages of highly differentiated calc-alkaline and alkaline granites, potassic volcanic rocks, and peralkaline intrusions also represent magmatic activity in a shear zone geotectonic setting, where the orogenic belt was dominated by transcurrent faulting and evolved into a non-orogenic environment (Oyhantcabal et al., 2007). Under continuous extensional tectonic environments, multiple stages intrusive in shallow crust made the closely related field genesis of the Inexpressible Island syenite and diorite dyke, this is consistent with the results of previous studies on TeNIC petrography (Rocchi et al., 2004; Bomparola et al., 2007). If we consider that the Inexpressible syenite has a similar evolutionary relationship to the lamprophyres of the Vegetation Island extension to Inexpressible Island (called a diorite dyke in Inexpressible Island), the gross petrologic, geochemical, and geochronologic differences in the magmatism can be explained by alternating phases of extension and contraction in the overriding plate (Figure 13A). In northernmost northern Victoria Land, multiple continental and oceanic arcs were syn-tectonically active (Figure 13A). Rather, accretion alternated with the detachment of a continental material-laden forearc–backarc from the main margin (Rocchi et al., 2011). During the late Ross Orogeny, horizontal transcurrent convergence caused the collision of transient coupling between convergent plates locked in the subduction process, and the slab lost its horizontal velocity component, sank into the mantle, and rolled back (Rocchi et al., 2009) (Figure 13B). The rise of asthenosphere material that replaced ductile lithosphere exposed previously insulated portions of the mechanical boundary layer of the subcontinental mantle to asthenosphere mantle heating. The melting of the metasomatized thermal boundary layer of the subcontinental lithosphere gave way to the generation of diorite melts and subsequent syenites sources magma (Rocchi et al., 2011; Rocchi et al., 2015) Thus, we suggested that the ultrapotassic syenite may be the partial melting product of potassium-rich SCLM in this tectonic environment. The Inexpressible Island syenite formed from the evolved fraction of these melts (Figure 12). The emplacement of these rocks was probably controlled by some deep-seated fault/shear zones. Extension continued form late Cambrian to the early Ordovician Period. This period facilitated the upwelling of metasomatized SCLM derived sources and the emplacement of mafic rocks such as the Irizar diorite and Vegetation diorite, Inexpressible Island diorites (Figure 7A). The Inexpressible Island syenites probably formed from the same mafic magma through assimilation fractional crystallization (Figure 13).

In summary, we suggest that based on the tectonic and geochemical similarities of the Vegetation Island mafic rocks, Irizar granite dyke, Abbott gabbro, and granite with both late to post-orogenic shoshonites and lamprophyres (Turner, 1996; Turner and Foden, 1996; Di Vincenzo et al., 1997) coupled with field occurrence, age, and extensional emplacement regime suggest that the Inexpressible Island magmatism was linked to local involvement in the melting zone of an older previously enriched layer of the subcontinental lithospheric mantle, which was further metasomatized by a more recent subduction component.

Conclusion

1. The Inexpressible Island syenite samples (DJS-6 and DJS-13) zircon U-Pb ages are 471.8 ± 1.8 Ma (MSWD=0.87, *n*=20) and 477.3 ± 1.7 Ma (MSWD=0.59, n=20), respectively, indicating early Ordovician magmatic intrusive activity.
2. Whole-rock geochemistry shows that the Inexpressible Island syenite is weakly peraluminous metaluminous and ultra-potassium, with typical island-arc magmatic affinity. We interpret the syenite as an Ordovician intrusion associated with regional extensional in Wilson continental margin. The magma source is linked to local involvement in the melting zone of an older previously enriched layer of the subcontinental lithospheric mantle, which was further metasomatized by a more recent subduction component. Otherwise, plagioclase cumulate crystallization reflects the complex genesis of the magma source controlled by phlogopite and hornblende.
3. We support an active continental margin accretion model, which existed on the Antarctic margin of east Gondwana during the

Early Paleozoic, in which multiple plates and ocean arcs were active. Plate tectonic deformation led to slab roll-back or tear of subducted plates, and upwelling asthenosphere mantle activate the subcontinental lithospheric mantle beneath the continental arc, which components be modified by subduction component before, and the derived mantle magma is significantly more evolved, ultimately intrude in the current stratum, formed the Inexpressible Island syenite.

Data Availability Statement

The original contributions presented in the study are included in the article/Supplementary Material, further inquiries can be directed to the corresponding author.

Author contributions

LT contributed to conception and design of the study. PG organized the database. LC performed the statistical analysis. PG wrote the first draft of the manuscript. LT and LC wrote sections of the manuscript. All authors contributed to manuscript revision, read, and approved the submitted version.

Funding

This work was supported by the National Natural Science Foundation of China (No. 41976072), the Fundamental Research Funds for Second Institute of Oceanography, Ministry of Natural Resources (No. QNYC1901) and (No. JG2002).

Acknowledgments

We would like to acknowledge China's 34th Antarctic Scientific Expedition for help with the samples and investigation. Thanks are due to LT and LC for their guidance in the study and writing process. We are grateful to Dr. Eirini Poulaki and Dr. Giovanna Rizzo, and editor Gilby Jepson whose reviews have significantly improved this work.

Conflict of interest

The authors declare that the research was conducted in the absence of any commercial or financial relationships that could be construed as a potential conflict of interest.

Publisher's note

All claims expressed in this article are solely those of the authors and do not necessarily represent those of their affiliated organizations, or those of the publisher, the editors and the reviewers. Any product that may be evaluated in this article, or claim that may be made by its manufacturer, is not guaranteed or endorsed by the publisher.

Supplementary material

The Supplementary Material for this article can be found online at: https://www.frontiersin.org/articles/10.3389/feart.2022.966085/full#supplementary-material

References

Armienti, P., Ghezzo, C., Innocenti, F., Manetti, P., Rocchi, S., and Tonarini, S. (1990). Granite Harbour intrusives from north Victoria land between david and campbell glaciers: New geochronological data. *Zentralblatt für Geol. Paläontologie* 1, 63–74.

Arzamastsev, A. A., Bea, F., Glaznev, V. N., Arzamastseva, L. V., and Montero, P. (2001). Kola alkaline province in the paleozoic: Evaluation ofprimary mantle magma composition and magma generation conditions. *Russ. J. Earth Sci.* 3, 1–32. doi:10.2205/2001es000054

Bailey, D. K. (1987). "Mantle metasomatism—perspective and prospect," in *The alkaline rocks*. Editors J. G. Fitton and B. G. J. Upton (Oxford: Blackwell Scientific), 1–13.

Biagini, R., Cappelli, B., and Di Vincenzo, G. (1990). *P-T estimates of the Mt. Abbott intrusives and enclosed metamorphic "septa" at Terra Nova Bay*. North Victoria land, Antarctica: Vulcanismo potassico. *Ischia*.

Bird, P. (1979). Continental delamination and the Colorado plateau. *J. Geophys. Res.* 84, 7561–7571. doi:10.1029/jb084ib13p07561

Black, L. P., and Sheraton, J. W. (1990). The influence of Precambrian source components on the U-Pb zircon age of a Palaeozoic granite from northern Victoria Land, Antarctica. *Precambrian Res.* 46, 275–293. doi:10.1016/0301-9268(90)90016-J

Blichert-Toft, J., and Albarède, F. (1998). The Lu-Hf isotope geochemistry of chondrites and the evolu-tion of the mantle-crust system. *Earth Planet. Sci. Lett.* 148 (1-2), 349–258. doi:10.1016/s0012-821x(97)00198-2

Boger, S. (2011). Antarctica—Before and after Gondwana. *Gondwana Res.* 19, 335–371. doi:10.1016/j.gr.2010.09.003

Bomparola, R. M., Ghezzo, C., Belousova, E., Griffin, W. L., and O'Reilly, S. Y. (2007). Resetting of the U–Pb zircon system in cambro–ordovician intrusives of the deep freeze range, northern victoria land, Antarctica. *J. Petrology* 48, 327–364. doi:10.1093/petrology/egl064

Bonin, B. (2007). A-type granites and related rocks: Evolution of a concept, problems and prospects. *Lithos* 97 (1/2), 1–29. doi:10.1016/j.lithos.2006.12.007

Borg, S. G., and DePaolo, D. J. (1994). Laurentia, Australia, and Antarctica as a late Proterozoic supercontinent: Constraints from isotopic mapping. *Geology* 22, 307–310. doi:10.1130/0091-7613(1994)022<0307:laaaaa>2.3.co;2

Borg, S. G., Stump, E., Chappell, B. W., McCulloch, M. T., Wyborn, T., Armstrong, R. L., et al. (1987). Granitoids of northern victoria land, Antarctica: Implications of chemical and isotopic variations to regional crustal structure and tectonics. *Am. J. Sci.* 287, 127–169. doi:10.2475/ajs.287.2.127

Borg, S. G., Stump, E., and Holloway, J. R. (1986). Granitoids of northern victoria land, Antarctica: A reconnaissance study of field relations, petrography, and geochemistry. *Geol. Investigations North. Vic. Land* 46, 115–188. doi:10.1029/ar046p0115

Borsi, L., Petrini, R., Talarico, F., and Palmeri, R. (1995). Geochemistry and Sr-Nd isotopes of amphibolite dykes of northern Victoria Land, Antarctica. *Lithos* 35, 245–259. doi:10.1016/0024-4937(95)99070-d

Bracciali, L., Di Vincenzo, G., Rocchi, S., and Ghezzo, C. (2009). The Tiger Gabbro from northern Victoria Land, Antarctica: The roots of an island arc within the early Palaeozoic margin of Gondwana. *J. Geol. Soc. Lond.* 166, 711–724. doi:10.1144/0016-76492008-098

Bradshaw, J. D., and Laird, M. G. (1983). "The pre-Beacon geology of northern Victoria Land," in *Antarctic earth science*. Editor J. B. Jago (Canberra: Australian Academy of Science), 98–101.

Castelli, D., Lombardo, B., Oggiano, G., Rossetti, P., and Talarico, F. (1991). Granulite facies rocks of the Wilson terrane (northern victoria land): Campbell glacier. *Mem. della Soc. Geol. Ital.* 46, 197–203.

Cawood, P. A., and Buchan, C. (2007). Linking accretionary orogenesis with supercontinent assembly. *Earth-Science Rev.* 82 (3-4), 217–256. doi:10.1016/j.earscirev.2007.03.003

Cawood, P. A., Kroner, A., Collins, W. J., Kusky, T. M., Mooney, W. D., and Windley, B. F. (2009). Accretionary orogens through Earth history. *Geol. Soc. Lond. Spec. Publ.* 318, 1–36. doi:10.1144/sp318.1

Cawood, P. A. (2005). Terra australis orogen: Rodinia breakup and development of the pacific and iapetus margins of Gondwana during the neoproterozoic and paleozoic. *Earth-Science Rev.* 69, 249–279. doi:10.1016/j.earscirev.2004.09.001

Chen, H., Wang, W., and Zhao, Y. (2019). Constraints on early paleozoic magmatic processes and tectonic setting of inexpressible island, northern victoria land, Antarctica. *Adv. Polar Sci.* 30 (1), 52–69.

Condie, K. C., Beyer, E., Belousova, E., Griffin, W., and O'Reilly, S. Y. (2005). U–Pb isotopic ages and Hf isotopic composition of single zircons: The search for juvenile precambrian continental crust. *Precambrian Res.* 139, 42–100. doi:10.1016/j.precamres.2005.04.006

Condie, K. C. (2007). "Accretionary orogens in space and time,". Editors R. D. HatcherJr., M. P. Carlson, J. H. McBride, and J. R. Martínez Catalán (Geological Society of America), 200, 145–158.*4D Framew. Cont. Crust* Boulder, CO, United States.

Crispini, L., Di Vincenzo, G., and Palmeri, R. (2007). Petrology and 40Ar–39Ar dating of shear zones in the lanterman range (northern victoria land, Antarctica): Implications for metamorphic and temporal evolution at terrane boundaries. *Mineralogy Petrology* 89, 217–249. doi:10.1007/s00710-006-0164-2

Dalziel, I. W. D. (1992). Antarctica: A tale of two supercontinents? *Annu. Rev. Earth Planet. Sci.* 20, 501–526. doi:10.1146/annurev.ea.20.050192.002441

Dalziel, I. W. D. (1997). Overview: Neoproterozoic-Paleozoic geography and tectonics: Review, hypothesis, environmental speculation. *Geol. Soc. Am. Bull.* 109 (1), 16–42. doi:10.1130/0016-7606(1997)109<0016:onpgat>2.3.co;2

Davies, J. H., and von Blanckenburg, F. (1995). Slab breakoff: A model of lithosphere detachment and its test in the magmatism and deformation of collisional orogens. *Earth Planet. Sci. Lett.* 129, 85–102. doi:10.1016/0012-821x(94)00237-s

Di Vincenzo, G., Grande, A., and Rossetti, F. (2014). Paleozoic siliciclastic rocks from northern Victoria Land (Antarctica): Provenance, timing of deformation, and implications for the Antarctica–Australia connection. *Geol. Soc. Am. Bull.* 126, 1416–1438. doi:10.1130/b31034.1

Di Vincenzo, G., Rocchi, S., Ghezzo, C., and Andriessen, P. A. M. (1997a). "Felsic and mafic magmas in the Terra Nova intrusive complex (northern Victoria Land, Antarctica)," in *The antarctic region: Geological evolution and processes*. Editor C. A. Ricci (Siena: Terra Antartica Publications), 253–260.

Di Vincenzo, G., and Rocchi, S. (1999). Origin and interaction of mafic and felsic magmas in an evolving late orogenic setting: The Early Paleozoic Terra Nova Intrusive Complex, Antarctica. *Contributions Mineralogy Petrology* 137 (1-2), 15–35. doi:10.1007/s004100050579

Downes, H., Balaganskaya, E., Beard, A., Liferovich, R., and Demaiffe, D. (2005). Petrogenetic processes in the ultramafic, alkaline and carbonatitic magmatism in the kola alkaline province: A review. *Lithos* 85, 48–75. doi:10.1016/j.lithos.2005.03.020

Eby, G. N. (1992). Chemical subdivision of the A-type granitoids: Petrogenetic and tectonic implications. *Geol.* 20 (7), 641–644. doi:10.1130/0091-7613(1992)020<0641:csotat>2.3.co;2

Eby, G. N. (1990). The A-type granitoids: A review of their occurrence and chemical characteristics and speculations on their petrogenesis. *Lithos* 26 (1/2), 115–134. doi:10.1016/0024-4937(90)90043-z

Eggler, D. H. (1978). The effect of CO_2 upon partial melting of peridotite in the system Na_2O-CaO-Al_2O_3-MgO-SiO-CO_2 to 34 Kb. with an analysis of melting in a peridotite-H_2O-CO_2 system. *Am. J. Sci.* 278, 305–343. doi:10.2475/ajs.278.3.305

Elliot, D. H., and Fanning, C. M. (2008). Detrital zircons from upper permian and lower triassic victoria group sandstones, shackleton glacier region, Antarctica: Evidence for multiple sources along the Gondwana plate margin. *Gondwana Res.* 13, 259–274. doi:10.1016/j.gr.2007.05.003

Encarnación, J., and Grunow, A. (1996). Changing magmatic and tectonic styles along the paleo-Pacific margin of Gondwana and the onset of early Paleozoic magmatism in Antarctica. *Tectonics* 15, 1325–1341. doi:10.1029/96tc01484

Estrada, S., Läufer, A., Eckelmann, K., Hofmann, M., Gärtner, A., and Linnemann, U. (2016). Continuous neoproterozoic to ordovician sedimentation at the east Gondwana margin - implications from detrital zircons of the ross orogen in northern victoria land, Antarctica. *Gondwana Res.* 37, 426–448. doi:10.1016/j.gr.2015.10.006

Federico, L., Capponi, G., and Crispini, L. (2006). The ross orogeny of the transantarctic mountains: A northern victoria land perspective. *Int. J. Earth Sci.* 95 (5), 759–770. doi:10.1007/s00531-005-0063-5

Federico, L., Crispini, L., Capponi, G., and Bradshaw, J .D. (2009). The Cambrian ross orogeny in northern Victoria Land (Antarctica) and New Zealand: A synthesis. *Gondwana Research* 15 (2), 188–196. doi:10.1016/j.gr.2008.10.004

Fergusson, C. L., Henderson, R. A., Fanning, C. M., and Withnall, I. W. (2007). Detrital zircon ages in neoproterozoic to ordovician siliciclastic rocks, northeastern Australia: Implications for the tectonic history of the east Gondwana continental margin. *J. Geol. Soc. Lond.* 164, 215–225. doi:10.1144/0016-76492005-136

Finn, C., Moore, D., Damaske, D., and Mackey, T. (1999). Aeromagnetic legacy of early Paleozoic subduction along the Pacific margin of Gondwana. *Geol.* 27, 1087–1090. doi:10.1130/0091-7613(1999)027<1087:aloeps>2.3.co;2

Fioretti, A. M., Capponi, G., Black, L. P., Varne, R., and Visona, D. (2005). Surgeon island granite shrimp zircon ages: A clue for the cambrian tectonic setting and evolution of the palaeopacific margin of Gondwana (northern victoria land, Antarctica). *Terra nova.* 17, 242–249. doi:10.1111/j.1365-3121.2005.00606.x

Fitzsimons, I. C. W. (2003). "Proterozoic basement provinces of southern and southwestern Australia, and their correlation with Antarctica," in *Proterozoic east Gondwana: Supercontinent assembly and break-up*. Editor S. Dasgupta (London: Geological Society), 93–130.

Foley, S. F., Venturelli, G., Green, D. H., and Toscani, L. (1987). The ultrapotassic rocks: Characteristics, classification and constraints for petrogenetic models. *Earth. Sci. Rev.* 24, 81–134. doi:10.1016/0012-8252(87)90001-8

Furman, T., and Graham, D. (1999). Erosion of lithospheric mantle beneath the east african rift system: Geochemical evidence from the kivu volcanic province. *Lithos* 24, 237–262. doi:10.1016/s0024-4937(99)00031-6

Gao, P., Tang, L. M., Chen, L., Yuan, T., and YinXia, F. (2022). Geochronology and geochemistry of the dioritic rocks from the Inexpressible Island, Northern Victoria Land, Antarctica and their geological implications. *Acta Petrol. Sin.* 38 (3), 923–941. doi:10.18654/1000-0569/2022.03.19

Ghezzo, C., Baldelli, C., Biagini, L., Carmignani, L., Di Vincenzo, G., Gosso, G., et al. (1987). Granitoids from the david glacier-aviator glacier segment of the transantarctic mountains, north Victoria land, Antarctica. *Mem. della Soc. Geol. Ital.* 33, 143–159.

Goodge, J. W., Fanning, C. M., Norman, M. D., and Bennett, V. C. (2012). Temporal, isotopic and spatial relations of early Paleozoic Gondwana-margin arc magmatism, central Transantarctic Mountains, Antarctica. *J. Petrology* 53, 2027–2065. doi:10.1093/petrology/egs043

Goodge, J. W., and Fanning, C. M. (2002). "Precambrian crustal history of the Nimrod Group, central Transantarctic mountains," in *Proceedings of the 8th international symposium on antarctic earth sciences*. Editors J. A. Gamble, D. A. Skinner, and S. Henrys (Wellington: Royal Society of New Zealand Bulletin), 43–50.

Goodge, J. W. (2020). Geological and tectonic evolution of the Transantarctic Mountains, from ancient craton to recent enigma. *Gondwana Res.* 80, 50–122. doi:10.1016/j.gr.2019.11.001

Goodge, J. W., Williams, I. S., and Myrow, P. (2004). Provenance of Neoproterozoic and lower Paleozoic siliciclastic rocks of the central Ross orogen, Antarctica: Detrital record of rift-passive-and active-margin sedimentation. *Geol. Soc. Am. Bull.* 116, 1253–1279. doi:10.1130/b25347.1

Grew, E. S., and Sandiford, M. (1984). A staurolite-talc assemblage in tourmaline-phlogopite-chlorite schist from northern Victoria Land, Antarctica, and its petrogenetic significance. *Contr. Mineral. Pet.* 87 (4), 337–350. doi:10.1007/bf00381290

Gunn, G. M., and Warren, G. (1962). Geology of victoria land between mawson and mullock glaciers, Antarctica. *N. Z. Geol. Surv. Bull.* 71, 157.

Hagen-Peter, G., and Cottle, J. M. (2016). Synchronous alkaline and subalkaline magmatism during the late neoproterozoic–early paleozoic ross orogeny, Antarctica: Insights into magmatic sources and processes within a continental arc. *Lithos* 262, 677–698. doi:10.1016/j.lithos.2016.07.032

Hagen-Peter, G., Cottle, J. M., Tulloch, A. J., and Cox, S. C. (2015). Mixing between enriched lithospheric mantle and crustal components in a short-lived subduction-related magma system, dry valleys area, Antarctica: Insights from U-Pb geochronology, Hf isotopes, and whole-rock geochemistry. *Lithosphere* 7, 174–188. doi:10.1130/l384.1

HartStanley, R. (1984). A large-scale isotope anomaly in the southern hemisphere mantle. *Nature* 309 (5971), 753–757. doi:10.1038/309753a0

Hoskin, P. W., and Schaltegger, U. (2003). The composition of zircon and igneous and metamorphic petrogenesis. *Rev. Mineral. Geochem.* 53, 27–62. doi:10.2113/0530027

Houseman, G. A., McKenzie, D. P., and Molnar, P. J. (1981). Convective instability of a thickened boundary layer and its relevance for the thermal evolution of continental convergent belts. *J. Geophys. Res.* 86, 6115–6132. doi:10.1029/jb086ib07p06115

Hu, Z. C., Liu, Y. S., Gao, S., Liu, W., Yang, L., Zhang, W., et al. (2012). Improved *in situ* Hf isotope ratio analysis of zircon using newly designed X skimmer cone and Jet sample cone in combination with the addition of nitrogen by laser ablation multiple collector ICP-MS. *J. Anal. At. Spectrom.* 27, 1391–1399. doi:10.1039/c2ja30078h

Jackson, S. E., Pearson, N. J., Griffin, W. L., and Belousova, E. A. (2004). The application of laser ablation-inductively coupled plasma-mass spectrometry to in situ U-Pb zircon geochronology. *Chemical Geology* 211, 47–69. doi:10.1016/j.chemgeo.2004.06.017

Jacobs, J., and Thomas, R. J. (2004). Himalayan-type indenterescape tectonics model for the southern part of the late Neoproterozoic–early Paleozoic East African–Antarctic orogen. *Geol.* 32 (8), 721–724. doi:10.1130/G20516.1

Jahn, B. M., Wu, F., Lo, C. H., and Tsai, C. H. (1999). Crust–mantle interaction induced by deep subduction of the continental crust: Geochemical and Sr–Nd isotopic evidence from post-collisional mafic–ultramafic intrusions of the northern dabie complex, central China. *Chem. Geol.* 157 (1-2), 119–146. doi:10.1016/s0009-2541(98)00197-1

Janosy, R. J., and Wilson, T. J. (1995). "Tectonic setting of the early Paleozoic dike swarm in southern Victoria Land," in *VII international symposium on antarctic earth sciences abstracts*. Editor C. A. Ricci (Siena, Italy: Terra Antartica Publications).

Kleinschmidt, G., and Tessensohn, F. (1987). Early paleozoic westward directed subduction at the pacific continental margin of Antarctica, sixth Gondwana symposium. *Geophys. Monogr.* 105, 89. doi:10.1029/GM040p0089

Köksal, S., Romer, R. L., Göncüoglu, M. C., Romer, R. L., and Toksoy-Köksal, F. (2004). Timing of post-collisional H-type to A-type granitic magmatism: U-Pb titanite ages from the alpine central anatolian granitoids (Turkey). *Int. J. Earth Sci.* 93, 974–989. doi:10.1007/s00531-004-0432-5

Kretz, R. (1983). Symbols for rock-forming minerals. *Am. Mineralogist* 68 (1-2), 277–279.

Läufer, A., Lisker, F., and Phillips, G. (2011). Late ross-orogenic deformation of basement rocks in the northern deep freeze range, victoria land, Antarctica: The lichen hills shear zone. *Polarforschung* 80 (2), 60–70.

Li, C. F., Li, X. H., Li, Q. L., Guo, J. H., and Yang, Y. H. (2012). Rapid and precise determination of sr and nd isotopic ratios in geological samples from the same filament loading by thermal ionization mass spectrometry employing a single-step separation scheme. *Anal. Chim. Acta* 727 (10), 54–60. doi:10.1016/j.aca.2012.03.040

Li, S. Z., Yang, Z., and Zhao, S. J. (2016). Global early paleozoic orogen (II): Subduction accretionary type Orogeny.Journal of jilin university. *Earth Sci. Ed.* (464), 968–1004.

Liégeois, J. P., and Black, R. (1987). "Alkaline magmatism subsequent to collision in the Pan-African belt of the Adrar des Iforas (Mali),". Editors J. G. Fitton and B. J. G. Upton (London: Geological Society Special Publication), 30, 381–401.*Alkaline Igneous Rocks*

Liu, Y. S., Gao, S., Hu, Z. C., Gao, C. G., Zong, K. Q., and Wang, D. B. (2010). Continental and oceanic crust recycling-induced melt-peridotite interactions in the trans-north China orogen: U-Pb dating, Hf isotopes and trace elements in zircons from mantle xenoliths. *J. Petrology* 51 (1–2), 537–571. doi:10.1093/petrology/egp082

Liu, Y. S., Hu, Z. C., Gao, S., Günther, D., Xu, J., Gao, C. G., et al. (2008). *In situ* analysis of major and trace elements of anhydrous minerals by LA-ICP-MS without applying an internal standard. *Chem. Geol.* 257 (1-2), 34–43. doi:10.1016/j.chemgeo.2008.08.004

Ludwig, K. R. (2003). A geochronological toolkit for microsoft excel. *ISOPLOT* 2003, 39.

Maniar, P. D., and Piccoli, P. M. (1989). Tectonic discrimination of granitoids. *Geol. Soc. Am. Bull.* 101 (5), 635–643. doi:10.1130/0016-7606(1989)101<0635:tdog>2.3.co;2

Middlemost, E. A. K. (1994). Naming materials in the magma/igneous rock system. *Earth. Sci. Rev.* 37, 215–224. doi:10.1016/0012-8252(94)90029-9

Moores, E. M. (1991). Southwest U.S. - east Antarctic (SWEAT) connection: A hypothesis. *Geol.* 19, 425–428. doi:10.1130/0091-7613(1991)019<0425:suseas>2.3.co;2

Nasdala, L., Lengauer, C. L., Hanchar, J. M., Kronz, A., Wirth, R., Blanc, P., et al. (2002). Annealing radiation damage and the recovery of cathodoluminescence. *Chem. Geol.* 191 (1-3), 121–140. doi:10.1016/s0009-2541(02)00152-3

Nelson, D. R., Mcculloch, M. T., and Sun, S. S. (1986). The origins of ultrapotassic rocks as inferred from Sr, Nd and Pb isotopes. *Geochimica Cosmochimica Acta* 50 (2), 231–245. doi:10.1016/0016-7037(86)90172-9

Niu, Y. L., and O'Hara, M. J. (2009). MORB mantle hosts the missing Eu (Sr, Nb, Ta and Ti) in the continental crust: New perspectives on crustal growth, crust-mantle differentiation and chemical structure of oceanic upper mantle. *Lithos* 112 (1/2), 1–17. doi:10.1016/j.lithos.2008.12.009

Oyhantcabal, P., Siegesmund, S., Wemmer, K., Frei, R., and Layer, P. (2007). Post-collisional transition from calc-alkaline to alkaline magmatism during transcurrent deformation in the southernmost Dom Feliciano belt (Braziliano–Pan-African, Uruguay). *Lithos* 98, 141–159. doi:10.1016/j.lithos.2007.03.001

Palmeri, R. (1997). P-T paths and migmatite formation: An example from Deep Freeze range, northern Victoria Land, Antarctica. *Lithos* 42, 47–66. doi:10.1016/s0024-4937(97)00036-4

Palmeri, R., Pertusati, P. C., Ricci, C. A., and Talarico, F. (1994). Late proterozoic (?)-early paleozoic evolution of the active pacific margin of Gondwana: Evidence from the southern Wilson terrane (northern victoria land, Antarctica). *Terra Antarct.* 1, 5–9.

Paulsen, T. S., Encarnación, J., Grunow, A. M., Layer, P. W., and Watkeys, M. (2007). New age constraints for a short pulse in Ross orogen deformation triggered by East-West Gondwana suturing. *Gondwana Res.* 12, 417–427. doi:10.1016/j.gr.2007.05.011

Pearce, J. A., Harris, N. B., and Tindle, A. G. (1984). Trace element discrimination diagrams for the tectonic interpretation of granitic rocks. *J. Petrology* 25, 956–983. doi:10.1093/petrology/25.4.956

Peccerillo, A., and Taylor, S. R. (1976). Geochemistry of eocene calc-alkaline volcanic rocks from the kastamonu area, northern Turkey. *Contr. Mineral. Pet.* 58 (1), 63–81. doi:10.1007/bf00384745

Perugini, D., Poli, G., and Rocchi, S. (2005). Development of viscous fingering between mafic and felsic magmas: Evidence from the Terra Nova intrusive complex (Antarctica). *Mineral. Pet.* 83, 151–166. doi:10.1007/s00710-004-0064-2

Pisarevsky, S. A., Wingate, M. D. T., Powell, C. M., Johnson, S., and Evans, D. A. D. (2003). "Models of Rodinia assembly and fragmentation," in *Proterozoic east Gondwana: Supercontinent assembly and break-up*. Editor S. Dasgupta (London: Geological Society), 35–55.

Rocchi, S., Bracciali, L., Di Vincenzo, G., Gemelli, M., and Ghezzo, C. (2011). Arc accretion to the early paleozoic antarctic margin of Gondwana in victoria land. *Gondwana Res.* 19, 594–607. doi:10.1016/j.gr.2010.08.001

Rocchi, S., Di Vincenzo, G., Ghezzo, C., and Nardini, I. (2009). Granite–lamprophyre connection in the latest stages of the early paleozoic ross orogeny (victoria land, Antarctica). *Geol. Soc. Am. Bull.* 121, 801–819. doi:10.1130/b26342.1

Rocchi, S., Di Vincenzo, G., and Ghezzo, C. (2004). The Terra Nova intrusive complex (victoria land, Antarctica), with 1:50, 000 geopetrographic map. *Terra Antarct. Rep.* 10, 51.

Rocchi, S., Tonarini, S., Armienti, P., Innocenti, F., and Manetti, P. (1998). Geochemical and isotopic structure of the early Palaeozoic active margin of Gondwana in northern Victoria Land, Antarctica. *Tectonophysics* 284, 261–281. doi:10.1016/s0040-1951(97)00178-9

Rocchi, S., Vincenzo, G. D., Dini, A., Petrelli, M., and Vezzoni, S. (2015). Time-space focused intrusion of genetically unrelated arc magmas in the early paleozoic ross-delamerian orogen (morozumi range, Antarctica). *Lithos* 232, 84–99. doi:10.1016/j.lithos.2015.06.006

Rossetti, F., Tecce, F., Aldega, L., Brilli, M., and Faccenna, C. (2006b). Deformation and fluid flow during orogeny at the palaeo-pacific active margin of Gondwana: The early palaeozoic Robertson Bay accretionary complex (North Victoria land, Antarctica). *J. Metamorph. Geol.* 24, 33–53. doi:10.1111/j.1525-1314.2005.00620.x

Rossetti, F., Vignaroli, G., Di Vincenzo, G., Gerdes, A., Ghezzo, C., Theye, T., et al. (2011). Long-lived orogenic construction along the paleo-pacific margin of Gondwana (deep freeze range, north Victoria land, Antarctica). *Tectonics* 30. doi:10.1029/2010tc002804

Rubatto, D., and Gebauer, D. (2000). *Use of cathodoluminescence for U-Pb zircon dating by ion microprobe: Some examples from the western cathodoluminescence in geosciences*. Berlin, Heidelberg: Springer, 373–400.

Rubatto, D., and Hermann, J. (2007). Experimental zircon/melt and zircon/garnet trace element partitioning and implications for the geochronology of crustal rocks. *Chem. Geol.* 241 (1-2), 38–61. doi:10.1016/j.chemgeo.2007.01.027

Rudnick, R. L., and Fountain, D. M. (1995). Nature and composition of the continental crust: A lower crustal perspective. *Rev. Geophys.* 33, 267–309. doi:10.1029/95rg01302

Rudnick, R. L., and Gao, S. (2003). Composition of the continental crust. *Treatise Geochem.* 3, 1–64. doi:10.1016/b0-08-043751-6/03016-4

Serri, G., Innocenti, F., and Manetti, P. (1993). Geochemical and petrological evidence of the subduction of delaminated Adriatic continental lithosphere in the Genesis of the Neogene-quaternary magmatism of Central Italy. *Tectonophysics* 223, 117–147. doi:10.1016/0040-1951(93)90161-c

Shellnutt, J. G., Wang, C. Y., Zhou, M. F., and Yang, Y. (2009). Zircon Lu-Hf isotopic compositions of metaluminous and peralkaline A-type granitic plutons of the emeishan large igneous province (SW China): Constraints on the mantle source. *J. Asian Earth Sci.* 35 (1), 45–55. doi:10.1016/j.jseaes.2008.12.003

Shellnutt, J. G., and Zhou, M. F. (2007). Permian peralkaline, peraluminous and metaluminous A-type granites in the panxi district, SW China: Their relationship to the emeishan mantle plume. *Chem. Geol.* 243 (3/4), 286–316. doi:10.1016/j.chemgeo.2007.05.022

Sláma, J., Košler, J., Condon, D. J., Crowley, J. L., Gerdes, A., Hanchar, J. M., et al. (2008). Plešovice zircon-A new natural reference material for U-Pb and Hf isotopic microanalysis. *Chem. Geol.* 249 (1–2), 1–35. doi:10.1016/j.chemgeo.2007.05.022

Steiger, R. H., and Jager, E. (1977). Subcommission on geochronology: Convention on the use of decay constants in geo- and cosmochronology. *Earth Planet. Sci. Lett.* 36 (3), 359–362. doi:10.1016/0012-821X(77)90060-7

Stump, E. (1995). *The Ross orogen of the transantarctic Mountains*. Cambridge University Press, 284.

Stump, E., Gootee, B., and Talarico, F. (2003). *Proceedings of the IX international symposium of antarctic earth sciences*. PotsdamBerlin Heidelberg New York: Springer-Verlag, 181–190.

Stump, E., Laird, M. G., Bradshaw, J. D., Holloway, J. R., Borg, S. G., and Lapham, K. E. (1983). Bowers graben and associated tectonic features cross northern Victoria Land, Antarctica. *Nature* 304, 334–336. doi:10.1038/304334a0

Sun, S. S., and McDonough, W. F. (1989). "Chemical and isotopic systematics of oceanic basalts: Implications for mantle composition and processes," in *Magmatism in the ocean basins*. Editors A. D. Saunders and M. J. Norry (London: Geological Society of London Special Publication), 313–345.

Talarico, F., Borsi, L., and Lombardo, B. (1995). Relict granulites in the ross orogen of northern victoria land (Antarctica), II. Geochemistry and palaeo-tectonic implications. *Precambrian Res.* 75, 157–174. doi:10.1016/0301-9268(95)80004-2

Talarico, F., and Castelli, D. (1995). Relict granulites in the Ross orogen of northern Victoria Land (Antarctica), I. Field occurrence, petrography and metamorphic evolution. *Precambrian Res.* 75, 141–156. doi:10.1016/0301-9268(95)80003-z

Tanaka, T., Togashi, S., Kamioka, H., Amakawa, H., Kagami, H., Hamamoto, T., et al. (2000). Jndi-1: A neodymium isotopic reference in consistency with lajolla neodymium. *Chem. Geol.* 168 (168), 279–281. doi:10.1016/s0009-2541(00)00198-4

Taylor, S. R. (1977). island arc models and the composition of the continental crust. *Union Maurice Ewing Ser.* 1, 325–335.

Taylor, S. R., and McLennan, S. M. (1985). The continental crust: Its composition and evolution. *Blackwell, Geol.* 157 (1–2), 119–146.

Thirlwall, M. F. (1991). Long-term reproducibility of multicollector sr and nd isotope ratio analysis. *Chem. Geol.* 94 (2), 85–104. doi:10.1016/s0009-2541(10)80021-x

Tiepolo, M., and Tribuzio, R. (2008). Petrology and U-Pb zircon geochronology of amphibole-rich cumulates with sanukitic affinity from Husky Ridge (northern Victoria Land, Antarctica): Insights into the role of amphibole in the petrogenesis of subduction-related magmas. *J. Petrology* 49, 937–970. doi:10.1093/petrology/egn012

Tonarini, S., and Rocchi, S. (1994). Geochronology of cambro–ordovician intrusives in northern victoria land: A review. *Terra Antarct.* 1, 46–50.

Turner, S. P., and Foden, J. (1996)., 56. South Australia, 147–169. doi:10.1007/BF01162601Magma mingling in late-Delamerian A-type granites at Mannum, South Australia*Mineralogy Petrology*

Turner, S. P. (1996). Petrogenesis of the late Delamerian gabbroic complex at Black Hill, South Australia: Implications for convective thinning of the lithospheric mantle. *Mineralogy Petrology* 56, 51–89. doi:10.1007/BF01162657

Vaughan, A. P., and Pankhurst, R. J. (2008). Tectonic overview of the west Gondwana margin. *Gondwana Res.* 13 (2), 150–162. doi:10.1016/j.gr.2007.07.004

Vervoort, J. D., and Blichert-Toft, J. (1999). Evolution of the depleted mantle: Hf isotope evidence from juvenile rocks through time. *Geochimica Cosmochimica Acta* 63 (3-4), 533–556. doi:10.1016/s0016-7037(98)00274-9

Vetter, U., and Tessensohn, F. S., (1987). S- and I-type granitoids of North Victoria Land, Antarctica, and their inferred geotectonic setting. *Geol. Rundsch.* 76 (1), 233–243. doi:10.1007/bf01820585

Volkert, R. A., Feigenson, M. D., Patino, L. C., Delaney, J. S., and Ala Drake, A. J. (2000). Sr and Nd isotopic compositions, age and petrogenesis of A-type granitoids of the Vernon Supersuite, New Jersey Highlands, USA. *Lithos* 50, 325–347. doi:10.1016/S0024-4937(99)00065-1

Wang, R. R., Xu, Z. Q., Santosh, M., Liang, F., and Fu, X. (2017). Petrogenesis and tectonic implications of the early paleozoic intermediate and mafic intrusions in the south qinling belt, central China: Constraints from geochemistry, zircon U-Pb geochronology and Hf isotopes. *Tectonophysics* 712/713, 270–288. doi:10.1016/j.tecto.2017.05.021

Wang, W., Hu, J. m., Chen, H., Yu, G. W., Zhao, Y., and Liu, X. C. (2014). La-icp-ms Zircon U-Pb ages of the Inexpressible Island intrusive rocks in north Victoria, Antarctica and their geological implications. *Geol. Bull. China* 33 (12), 9.

Weaver, S. D., Bradshaw, J. D., and Laird, M. G. (1984). Geochemistry of cambrian volcanics of the Bowers supergroup and implications for the early palaeozoic tectonic evolution of northern victoria land, Antarctica. *Earth Planet. Sci. Lett.* 68, 128–140. doi:10.1016/0012-821x(84)90145-6

Weis, D., Kieffer, B., Maerschalk, C., Barling, J., Jong, J. D., Williams, G. A., et al. (2006). High-precision isotopic characterization of usgs reference materials by tims and mc-icp-ms. *Geochem. Geophys. Geosyst.* 7 (8), 139–149. doi:10.1029/2006gc001283

Wendlandt, R. F. (1984). "An experimental and theoretical analysis of partial melting in the system $KAlSiO_4$-CaO-MgO-SiO_2-CO_2 and applications to the Genesis of potassic magmas. carbonatites and kimberlites," in *Kimberlites and related rocks*. Editor J. KRONPROBST, 359–369.

Whalen, J. B., Currie, K. L., and Chappell, B. W. (1987). A-type granites: Geochemical characteristics, discrimination and petrogenesis. *Contrib. Mineral. Pet.* 95 (4), 407–419. doi:10.1007/bf00402202

Whalen, J. B., McNicoll, V. J., van Staal, C. R., Lissenberg, C. J., Longstaffe, F. J., Jenner, G. A., et al. (2006). Spatial, temporal and geochemical characteristics of Silurian collision-zone magmatism, Newfoundland Appalachians: An example of a rapidly evolving magmatic system related to slab break-off. *Lithos* 89, 377–404. doi:10.1016/j.lithos.2005.12.011

Wilson, M., Downes, H., and Cebriá, J. M. (1995). Contrasting fractionation trends in coexisting continental alkaline magma series; cantal, massif central, France. *J. Petrology* 36, 1729–1753.

Wu, F. Y., Sun, D. Y., Li, H. M., Jahn, B. m., and Wilde, S. (2002). A-type granites in northeastern China: Age and geochemical constraints on their petrogenesis. *Chem. Geol.* 187 (1/2), 143–173. doi:10.1016/s0009-2541(02)00018-9

Wu, R. X., Zheng, Y. F., Wu, Y. B., Zhao, Z. F., Zhang, S. B., Liu, X. M., et al. (2006). Reworking of juvenile crust: Element and isotope evidence from neoproterozoic granodiorite in south China. *Precambrian Res.* 146, 179–212. doi:10.1016/j.precamres.2006.01.012

Wu, Y. B., and Zheng, Y. F. (2004). Genesis of zircon and its constraints on interpretation of U-Pb age. *Chin. Sci. Bull.* 49 (15), 1554–1569. doi:10.1360/04wd0130

Yang, J. H., Sun, J. F., Zhang, M., Wu, F. Y., and Wilde, S. A. (2012). Petrogenesis of silica-saturated and silica-undersaturated syenites in the Northern North China Craton related to post-collisional and intraplate extension. *Chem. Geol.* 328, 149–167. doi:10.1016/j.chemgeo.2011.09.011

Zhang, W., Hu, Z. C., and Liu, Y. S. (2020). Iso-compass: New freeware software for isotopic data reduction of LA-MC-ICP-MS. *J. Anal. At. Spectrom.* 35, 1087–1096. doi:10.1039/d0ja00084a

Zhang, W., and Hu, Z. (2020). Estimation of isotopic reference values for pure materials and geological reference materials. *At. Spectrosc.* 41 (3), 93–102. doi:10.46770/as.2020.03.001

Zheng, Y. F., Zhang, S. B., Zhao, Z. F., Wu, Y. B., Li, X. H., Li, Z. X., et al. (2007). Contrasting zircon Hf and O isotopes in the two episodes of neoproterozoic granitoids in south China: Implications for growth and reworking of continental crust. *Lithos* 96, 127–150. doi:10.1016/j.lithos.2006.10.003

Zong, K. Q., Klemd, R., Yuan, Y., He, Z. Y., Guo, J. L., Shi, X. L., et al. (2017). The assembly of Rodinia: The correlation of early Neoproterozoic (ca. 900 Ma) high-grade metamorphism and continental arc formation in the southern Beishan Orogen, southern Central Asian Orogenic Belt (CAOB). *Precambrian Res.* 290, 32–48. doi:10.1016/j.precamres.2016.12.010